A matrix metalloproteinase mediates long-distance attenuation of stem cell proliferation

Xiaoxi Wang[1,2] and Andrea Page-McCaw[1,2,3]

[1]Department of Cell and Developmental Biology, [2]Program in Developmental Biology, and [3]Department of Cancer Biology, Vanderbilt University Medical Center, Nashville, TN 37232

Ligand-based signaling can potentiate communication between neighboring cells and between cells separated by large distances. In the *Drosophila melanogaster* ovary, Wingless (Wg) promotes proliferation of follicle stem cells located ∼50 µm or five cell diameters away from the Wg source. How Wg traverses this distance is unclear. We find that this long-range signaling requires Division abnormally delayed (Dally)-like (Dlp), a glypican known to extend the range of Wg ligand in the wing disc by binding Wg. Dlp-mediated spreading of Wg to follicle stem cells is opposed by the extracellular protease Mmp2, which cleaved Dlp in cell culture, triggering its relocalization such that Dlp no longer contacted Wg protein. *Mmp2*-deficient ovaries displayed increased Wg distribution, activity, and stem cell proliferation. Mmp2 protein is expressed in the same cells that produce Wg; thus, niche cells produce both a long-range stem cell proliferation factor and a negative regulator of its spreading. This system could allow for spatial control of Wg signaling to targets at different distances from the source.

Introduction

Stem cells are supported by microenvironments called niches, which provide a combination of soluble signals and physical interactions to regulate stem cell behaviors. Although in many cases niche cells abut the stem cells directly, many stem cell regulatory factors, such as bone morphogenetic proteins (BMPs), Hedgehog, and Wnt, can signal over long ranges in other developmental contexts (Rogers and Schier, 2011). Indeed, the intersection patterns of long-range signaling molecules may define the spatial positioning of stem cells within a tissue; this appears to be the case for *Drosophila melanogaster* follicle stem cells (FSCs; Vied et al., 2012) and perhaps for stem cells of the mammalian olfactory epithelium (for review see Lander et al., 2012). The potential for long-range signaling molecules to regulate stem cell behaviors has implications in tumor progression and metastasis: the greater the range of heterotypic signals, the larger the potential tumor microenvironment for both primary and secondary tumors (Hanahan and Weinberg, 2011).

Correspondence to Andrea Page-McCaw: andrea.page-mccaw@vanderbilt.edu

Abbreviations used in this paper: Arm, Armadillo; BAC, bacterial artificial chromosome; BMP, bone morphogenetic protein; Dally, division abnormally delayed; Dlp, Dally-like protein; DSHB, Developmental Studies Hybridoma Bank; EMS, ethyl methanesulfonate; FSC, follicle stem cell; fz3, frizzled 3; GAG, glycosaminoglycan; GPI, glycosylphosphatidylinositol; GSC, germline stem cell; Hh, Hedgehog; hsFLP, heat shock-induced Flippase; MMP, matrix metalloproteinase; Ptc, Patched; RFP, red fluorescent protein; TF, terminal filament; Timp, tissue inhibitor of metalloproteinase; ts, temperature sensitive; Wg, Wingless.

Both mammalian and *Drosophila* ovaries contain somatic stem cells that give rise to differentiated cells encapsulating the developing germ cells (Margolis and Spradling, 1995; Fleskes-Nikitin et al., 2013). In the fly ovary, each germarium contains two FSCs, which give rise to a monolayer follicle epithelium encasing each developing egg (Fig. 1 A; Margolis and Spradling, 1995; Nystul and Spradling, 2007; Nystul and Spradling, 2010). After the initial stem cell division, daughters become follicle precursor cells, transit-amplifying cells that actively proliferate before differentiating into three cell types: stalk cells and polar cells, both of which immediately exit mitosis, and encasing follicle cells that proliferate through stage 6 (Horne-Badovinac and Bilder, 2005). FSCs are positioned midway along the germarium, and they appear to be approximately five cell diameters (∼50 µm) away from the cells that produce signaling ligands (Wingless [Wg] and Hedgehog [Hh]) regulating their behavior. Thus, FSCs are subject to long-range stem cell regulation (Forbes et al., 1996a,b; Song and Xie, 2003; Vied et al., 2012). Whether and how these signals traverse that distance is unclear (Sahai-Hernandez and Nystul, 2013).

In this study we establish a continuous path of Wg ligand and signaling activity emanating from the anterior end of the

The Rockefeller University Press $30.00
J. Cell Biol. Vol. 206 No. 7 923–936
www.jcb.org/cgi/doi/10.1083/jcb.201403084

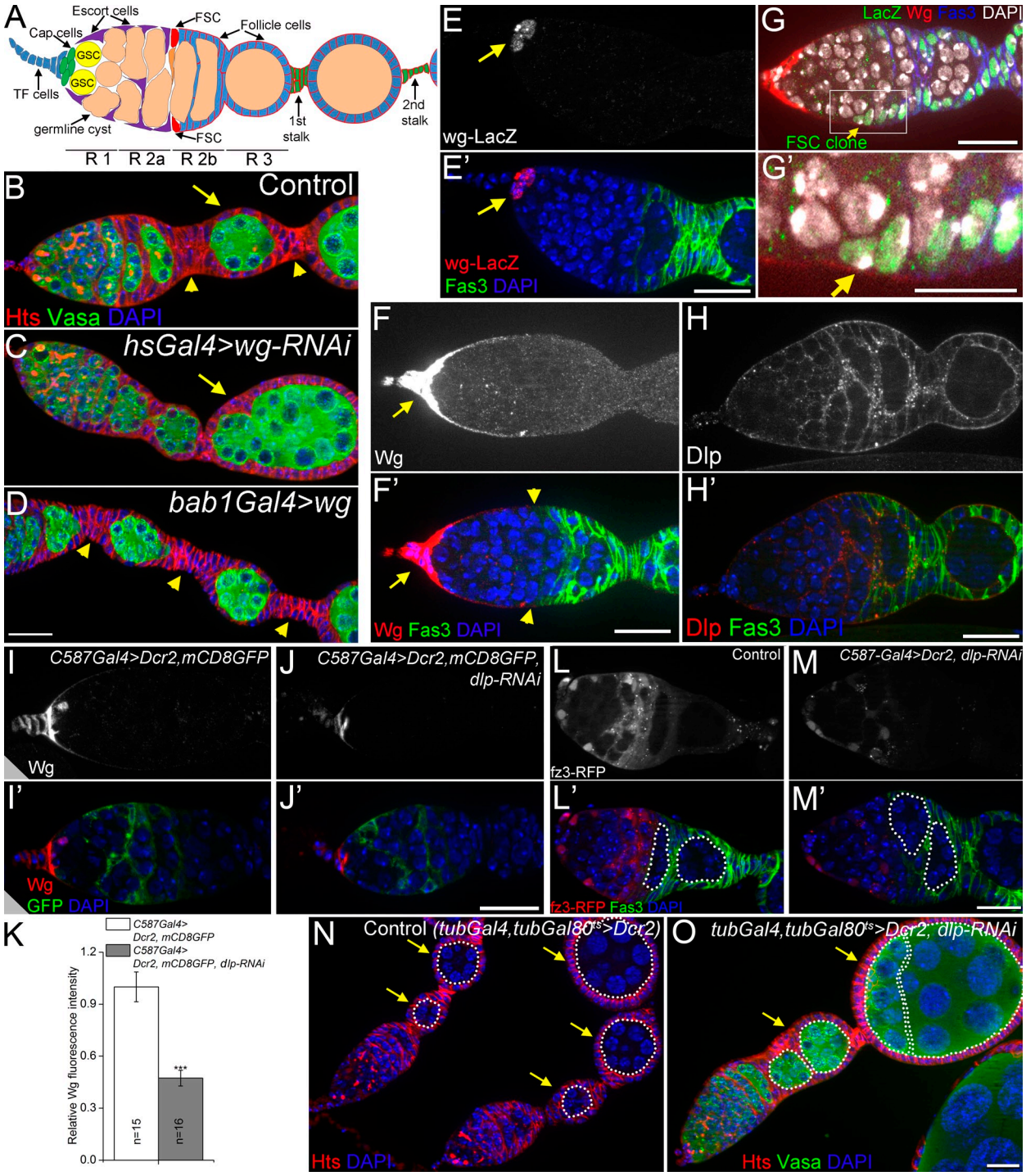

Figure 1. **Dlp promotes long-range Wg signaling to FSCs.** (A) A schematic diagram of the germarium. FSCs reside at the border of regions 2a (R 2a) and 2b. A cross-migrating FSC daughter is shown in orange. Follicle precursor cells are located in R 2b. TF cells (blue) and cap cells (green) are collectively called apical cells. GSC, germline stem cell. (B–D) Loss-of-function of *wg* (C) caused fused egg chambers (compound follicles, arrows; 60% penetration was observed in 35 ovarioles), whereas *wg* overexpression (D) resulted in stalks with increased cell numbers (arrowheads). (E) In wild-type germaria, *wg* was expressed only in cap cells (arrows) as shown by the *wg-lacZ* enhancer trap line. 3–5 cells were stained in 39/47 germaria. (F) In wild-type germaria, a continuous path of extracellular Wg (arrows), visualized at high exposure, spread to the FSCs (arrowheads). (G and G') Wg spreading to a *lacZ*-labeled FSC clone (arrows). (H) Anti-Dlp in wild-type germaria. (I–K) Loss of function of *dlp* (with RNAi) reduced the levels of anti-Wg extracellular staining. mCD8GFP shows the pattern of *C587Gal4* expression (strong in escort cells and weak in follicle cell precursors in region 2b). *Dicer-2* (*Dcr2*) enhanced RNAi efficiency. ***, $P < 0.001$ (Student's *t* test). Error bars represent SEM. *n* = number of germaria imaged. (L–M) *dlp* RNAi in escort cells decreased activity of the Wg signaling reporter *fz3-RFP* in posterior escort cells and FSCs, and caused encapsulation defects (58.3% of 84 germaria examined). 16-cell germline cysts in region 2b and region 3 are outlined. Note the two side-by-side cysts in *dlp* RNAi indicating an encapsulation defect. (N and O) Ubiquitous knockdown of *dlp* with *tubGal4* resulted in fused egg chambers in 22.1% of 68 *dlp* RNAi germaria (arrows in O), compared with 0% in 42 control germaria (N). 16-cell germline cysts are outlined, egg chambers are indicated by arrows. DAPI labels DNA in blue. Anti-Hts labels follicle cell plasma membranes, spectrosomes, and fusomes. Anti-Vasa labels the germline. Anti-Fas3 labels follicle cell borders. Bars: (G') 10 µm; (all other panels) 20 µm.

germarium and extending to the FSCs, which lie on the shallow end of this observed ligand gradient. When the amount of Wnt signal is increased from the source, the stem cell proliferation rate increases. We identify a positive and negative regulator of Wnt long-range signaling to the FSC, and these collaborate to regulate the level and distribution of ligand sensed by the FSCs. The positive regulator is the glypican Division abnormally delayed (Dally)-like protein (Dlp), known to promote the spreading of Wg ligand in the wing disc; the negative regulator is a matrix metalloproteinase (MMP), a novel antagonist of canonical Wnt signaling, expressed in cells of the FSC niche. As a Wnt signaling antagonist, the MMP cleaves the glypican, reducing the ability of Dlp to interact with the Wnt ligand and promote its distribution. Thus, the niche produces both a long-range proliferative signal and the machinery to regulate the distribution of that signal.

Results

Long-distance Wg signaling promotes FSC proliferation

Wnt signaling regulates proliferation and self-renewal in many types of stem cells across species (de Lau et al., 2007; Clevers and Nusse, 2012). The Wnt ligand is understood to act at short range, signaling to a stem cell from a neighboring cell source. However, in the *Drosophila* ovary, the relationship between the Wnt ligand and FSC proliferation is unclear because of the distance between them. FSC proliferation can be assessed by stalk cell number: in mutants where the FSCs over-proliferate, excess cells are shunted off to the stalks where they stop proliferating, resulting in increased numbers of stalk cells between egg chambers; in contrast, fewer FSC divisions result in not enough follicle cells, so that egg chambers are fused with fewer or no stalk cells (Forbes et al., 1996a; Song and Xie, 2003). Wnt downstream signaling is required for normal FSC proliferation, as ectopic activation of the Wnt pathway in FSCs (through loss of *Axin* or *shaggy*) triggers excess stalk cells, and loss of canonical Wnt signaling components (*dishevelled* or *armadillo* [*arm*]/*β-catenin*) autonomously in the FSCs results in stem cell loss (Song and Xie, 2003). We confirmed the role of the Wg ligand (one of seven Wnts in *Drosophila*) in FSC proliferation: RNAi-mediated loss of Wg resulted in fused egg chambers typical of reduced FSC proliferation (Fig. 1, B and C; Song and Xie, 2003). Conversely, overexpression of Wg in the somatic cells with *bab1Gal4* (FBal0242651; Bolívar et al., 2006) resulted in increased stalk cell numbers (Fig. 1, B and D). As others have observed, *wg* transcription was limited to the apical cells (Fig. 1 E; Forbes et al., 1996b), raising the question of how—or even whether—this ligand can traverse the 50-µm distance between the source and the FSCs. We stained germaria for extracellular Wg protein, and, consistent with previous studies (Song and Xie, 2003), Wg protein was most abundant around the apical cells (arrows in Fig. 1 F). However, at high exposures we observed Wg protein in a continuous path extending to the FSCs (arrowheads in Fig. 1 F′; see Fig. S1 for antibody specificity control). Although there is no reliable marker for FSCs, they were unambiguously identified by lineage tracing (Fig. 1, G and G′, arrows). This direct visualization strongly suggested that Wg directly regulates FSCs, rather than triggering a signaling relay.

Dlp promotes long-distance Wg signaling in the germarium

The best-understood example of long-distance Wg signaling is in the fly wing disc. In the wing, although Wg is produced in a thin stripe of cells, the extracellular protein is distributed over a distance of ∼50 µm (Strigini and Cohen, 2000). Recent work has called into question the requirement for Wg spreading in patterning the wing, as flies that have all Wg ligand tethered to the cell membrane still develop normally patterned wings; however, this work also demonstrates that long-distance Wg signaling is required for normal cell proliferation in the wing and has other functions outside the wing that increase fitness (Alexandre et al., 2014). The spreading of Wg away from its source in the wing requires the glypican Dlp, a heparan sulfate proteoglycan tethered to the cell surface by a glycosylphosphatidylinositol (GPI) anchor. Dlp promotes Wg signaling in cells far from the source while simultaneously reducing short-range Wg signaling (Baeg et al., 2004; Kirkpatrick et al., 2004; Kreuger et al., 2004; Franch-Marro et al., 2005). Dlp binds Wg in cell culture (Yan et al., 2009), and in the wing disc Dlp protects extracellular Wg from endocytosis and degradation, allowing more Wg to be used for long-range signaling (Marois et al., 2006). Although Dlp is not known to regulate stem cell function or Wg signaling in the ovary, we stained ovaries for Dlp and confirmed previous reports of Dlp expression in the germarium (Fig. 1 H; Guo and Wang, 2009; Hayashi et al., 2012). As in the wing disc, the pattern of Dlp staining was inverse to that of Wg ligand (compare Fig. 1, F and H; Han et al., 2005). To address whether Dlp promotes Wg distribution in the ovary, we took an RNAi approach, as *dlp* mutants are lethal. When *dlp* was knocked down within escort cells and early follicle cells (*C587-Gal4*), we observed a decrease in the total amount and the spread of extracellular Wg protein (Fig. 1, I–K). To determine the effect of Dlp on Wg signaling activity, we identified a Wg signaling reporter, as none has been characterized in the germarium. Testing seven candidate reporters from other tissues (Fig. S2), we identified *fz3-RFP*, which expresses red fluorescent protein (RFP) under the *frizzled 3* (*fz3*) promoter (Olson et al., 2011), as a Wg signaling reporter activated in a domain from the escort cells to the FSCs (Fig. 1 L), the same domain that contacts the Wg ligand we visualized (Fig. 1 F). We validated this reporter using mutations that turned on and off the Wg pathway (Fig. S2, A and B). In *dlp* knockdown germaria, this Wg activity domain was sharply reduced (Fig. 1 M). Importantly, loss of *dlp* also caused encapsulation defects (Fig. 1 M) and the appearance of compound follicles without intervening stalk cells (Fig. 1 O), similar to the *wg* LOF phenotype (Fig. 1 C). Thus, knockdown of *dlp* reduces Wg ligand spreading, Wg signaling, and stalk cell numbers. We conclude that Dlp promotes the spread of Wg from the apical cells to the FSCs.

Mmp2 limits long-distance Wg signaling in the germarium

Conditional mutations in the extracellular protease *Mmp2* also disrupted the number of follicle cells in ovarian stalks. Two

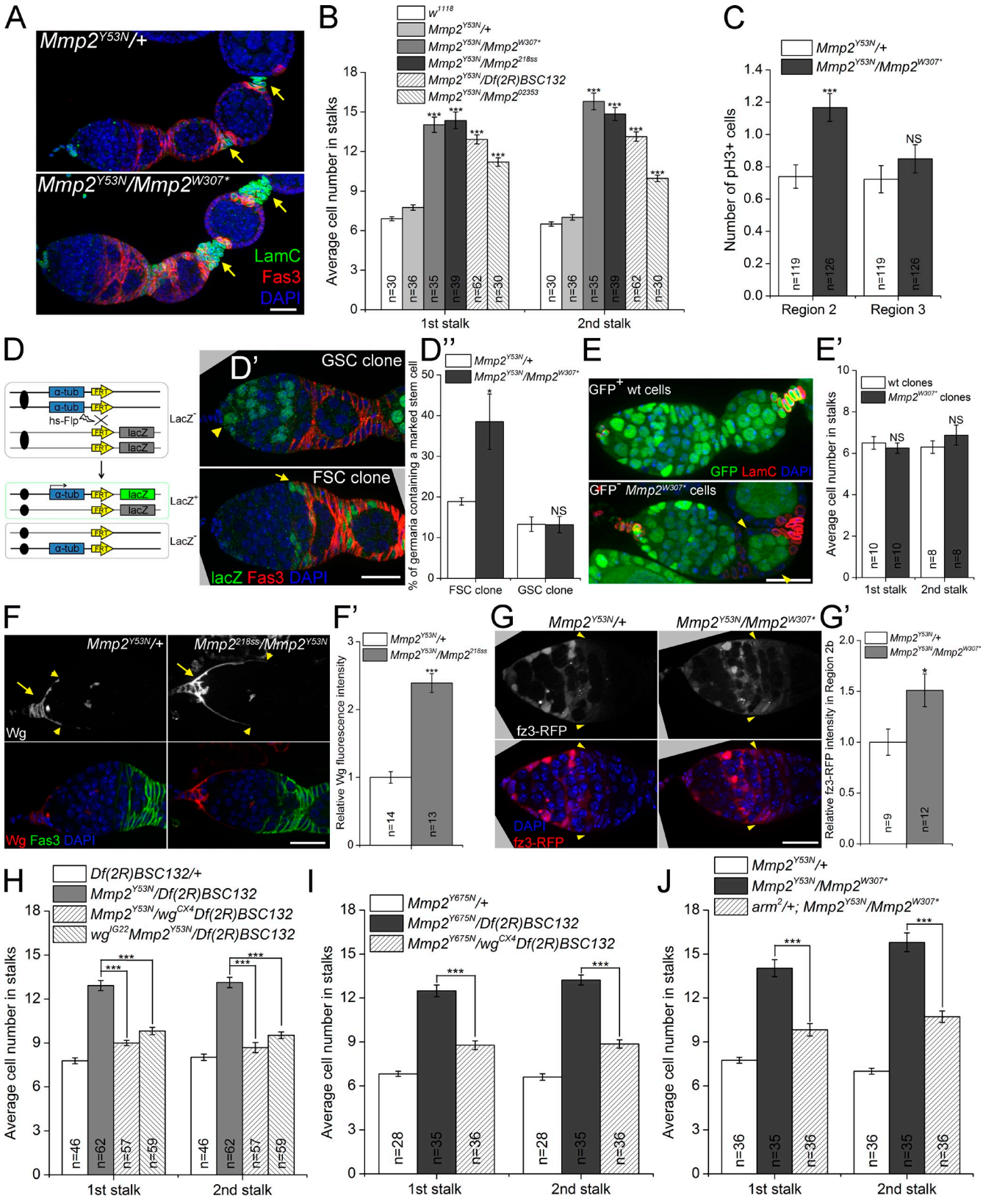

Figure 2. **Mmp2 restricts long-range Wg signaling to FSCs.** (A) *Mmp2* ts mutant ovaries had stalks with increased cell numbers at a nonpermissive temperature. Arrows, first and second stalks. (B) Quantification of stalk cell numbers in *Mmp2* ts mutants 7–9 d after temperature shift. Significance is relative to $Mmp2^{Y53N}/+$ controls. (C) *Mmp2* ts mutants showed increased proliferation of follicle precursor cells in region 2b. The number of mean pH3-positive follicle cells (including FSCs) per germarium is shown. (D–D″) FSCs divide more frequently in *Mmp2* ts mutants. (D) Scheme for lineage-marking mitotic cells: hsFlp recombines the α-tub promoter (blue) in cis with the *lacZ* ORF (green). (D′) A GSC clone (arrowhead) and an FSC clone (arrow), each positively marked by *lacZ* (green). (D″) The percentage of germaria with at least one $lacZ^+$ FSC clone or GSC clone for control and *Mmp2* ts mutants (four independent experiments). (E and E′) *Mmp2* was not required in follicle cells: $Mmp2^{w307*}$ mitotic clones (GFP-negative, arrowheads) had comparable stalk

temperature-sensitive (ts) alleles, $Mmp2^{Y53N}$ and $Mmp2^{Y675N}$ (Fig. S3 A), isolated in a previous ethyl methanesulfonate (EMS) screen (Page-McCaw et al., 2003) displayed conditional *Mmp2* phenotypes. When in trans to a strong *Mmp2* allele (ts mutants), both alleles were lethal at nonpermissive temperatures and viable at permissive temperatures (see Fig. S3 B). Ts mutant females showed reduced fertility after the switch to nonpermissive temperatures, and upon dissection, *Mmp2* ts mutant ovaries exhibited extra stalk cells (Fig. 2 A, arrows), with about twice as many cells in the first and second stalks as controls (Figs. 2 B and S3 C). Similar results were obtained for each *Mmp2* ts allele in trans to several strong alleles: $Mmp2^{W307*}$ and $Mmp2^{218ss}$ (EMS alleles, see Fig. S3 A), *Df(2R)BSC132* (a deletion removing the entire *Mmp2* gene), and $Mmp2^{02353}$ (P element insertion in the third intron; Page-McCaw et al., 2003; see Fig. S3 C for Y675N data). Phospho-histone H3 staining revealed increased follicle cell proliferation specifically in region 2b, where the stem and precursor cells reside, but not in later stages (Fig. 2 C). Thus, *Mmp2* appeared to inhibit early follicle cell proliferation.

This increase in follicle cell proliferation could be caused by an increase in stem cell divisions or by an increase in precursor cell divisions. To determine if stem cell divisions increased in *Mmp2* ts mutants, we analyzed the frequency of generating mitotic clones. Dividing cells and their descendants can be permanently labeled by a mitotic recombination lineage-tracing method shown in Fig. 2 D. In brief, heat shock-induced Flippase (hsFlp) triggers homologous recombination between two FRT sites during mitosis, bringing the α-tub promoter and *lacZ* ORF in cis, which turns on *lacZ* expression (Harrison and Perrimon, 1993). The frequency of *lacZ* labeling depends on the length of heat shock and the rate of cell division. Although recombination can occur in any mitotic cell, only recombination in stem cells results in a permanent labeling, visualized 1 wk after heat shock. The rate of mitotic recombination in FSCs was significantly increased in *Mmp2* mutants compared with heterozygote controls. In contrast, the incidence of mitotic labeling of germline stem cells (GSCs) did not change in mutants compared with controls (Fig. 2, D′ and D″). Thus, *Mmp2* negatively regulates the proliferation of FSCs in the germarium.

To determine if *Mmp2* was required in the follicle cells or stem cells to regulate FSC proliferation, we generated $Mmp2^{w307*}$ mitotic clones that included FSCs and the entire follicle epithelia. Despite the loss of *Mmp2* from these cells, no change in stalk cell number was found (Fig. 2, E and E′). Because Mmp2 did not act in follicle cells directly, we asked whether it limited FSC proliferation by regulating niche signals including Hh and Wg. After staining for extracellular Wg protein, we observed a clear increase in the level of extracellular Wg protein in *Mmp2* mutants compared with heterozygote controls, with the Wg distribution extending further posterior toward the FSCs (Fig. 2, F and F′, arrowheads). The *fz3-RFP* Wg signaling reporter confirmed increased Wg activity in FSCs and follicle precursor cells in region 2b in *Mmp2* ts mutants (Fig. 2, G and G′). *Mmp2* negatively regulated Wg levels through a posttranscriptional mechanism, as a *wg* transcriptional reporter (*wg-lacZ* enhancer trap) displayed lower rather than higher activity in *Mmp2* mutants, which indicates feedback regulation of *wg* transcription (Fig. S3 D). Although Hh signaling can also regulate FSC proliferation (Forbes et al., 1996a; Zhang and Kalderon, 2001), Hh signaling was not affected, as *Mmp2* mutants expressed comparable levels of the Hh reporter Patched (Ptc; Fig. S3 E). Thus, in *Mmp2* mutants, Wg signaling is increased, and FSCs increase their proliferation.

To determine if there is a causal link between increased Wg signaling and FSC overproliferation in *Mmp2* mutants, we asked if reducing the dose of *wg* suppressed the *Mmp2*-increased stalk cell numbers. Two independent alleles of *wg* (wg^{CX4} and wg^{IG22}) resulted in dominant suppression of stalk cell numbers when *wg* was heterozygous in several different *Mmp2* ts backgrounds (Fig. 2, H and I). Furthermore, mutating one copy of β-catenin (with the arm^{2} allele, which compromises Wg signaling activity without affecting adherens junctions; Cox et al., 1999) also suppressed the stalk cell phenotype of *Mmp2* mutants (Fig. 2 J), which indicates that *Mmp2* acts through canonical Wnt signaling to regulate FSC proliferation (Niehrs, 2012). Thus, Mmp2 limits Wg signaling to FSCs.

Mmp2 antagonizes Dlp in regulating long-range Wg signaling

We explored genetic interactions between *Mmp2* and *wg* in gain-of-function studies. Although adult onset of *Mmp2* overexpression with several different Gal4 drivers ($bab1Gal^{Agal4-5}$ and *ptcGal4*) resulted in lethality, we found that females could survive more than a week after $Gal80^{ts}$-based conditional overexpression with *C587-Gal4*, expressed strongly in escort cells and weakly in follicle precursor cells in region 2b (Fig. 1 I; Manseau et al., 1997; Kirilly et al., 2011). This *Mmp2* overexpression resulted in fused egg chambers lacking the stalk structure (Fig. 3, A, B, and F), which is reminiscent of *wg* loss of function (Fig. 1 C), supporting the model that *Mmp2* negatively regulates Wg. Furthermore, this negative regulation requires the proteolytic activity of Mmp2, as coexpression of tissue inhibitor of metalloproteinase (Timp) suppressed the fused egg chamber phenotype and rescued the stalk cell numbers to wild-type levels (Fig. 3, C and F). Interestingly, when *Mmp2* and *wg* were co-overexpressed, the stalk cell numbers were increased to an extent similar to when *wg* was overexpressed alone (Fig. 3, D–F). Thus, *wg* is epistatic to *Mmp2* in this system, which suggests that Mmp2 does not act directly on the Wg ligand. In support

cell numbers to *wt* controls. (F and F′) *Mmp2* ts mutants showed increased extracellular Wg staining in cap cells (arrows). Wg staining extended further in a posterior direction along the basement membrane (arrowheads denote the edge of visible Wg). F′ quantifies Wg intensity. (G and G′) *Mmp2* ts mutants had increased Wg signaling in FSCs (arrowheads) and follicle precursor cells, visualized by the *fz3-RFP* reporter. G′ quantifies fz3-RFP intensity in FSCs and follicle precursor cells in region 2b. (H–J) Reducing *wg* with either of two alleles (H and I) or *arm* (J) dominantly suppressed the increased stalk cell number in *Mmp2* ts mutants. *, $P < 0.05$; ***, $P < 0.001$; NS, not significant; Student's *t* test. Error bars represent SEM. *n* = number of germaria counted or imaged. Bars, 20 µm.

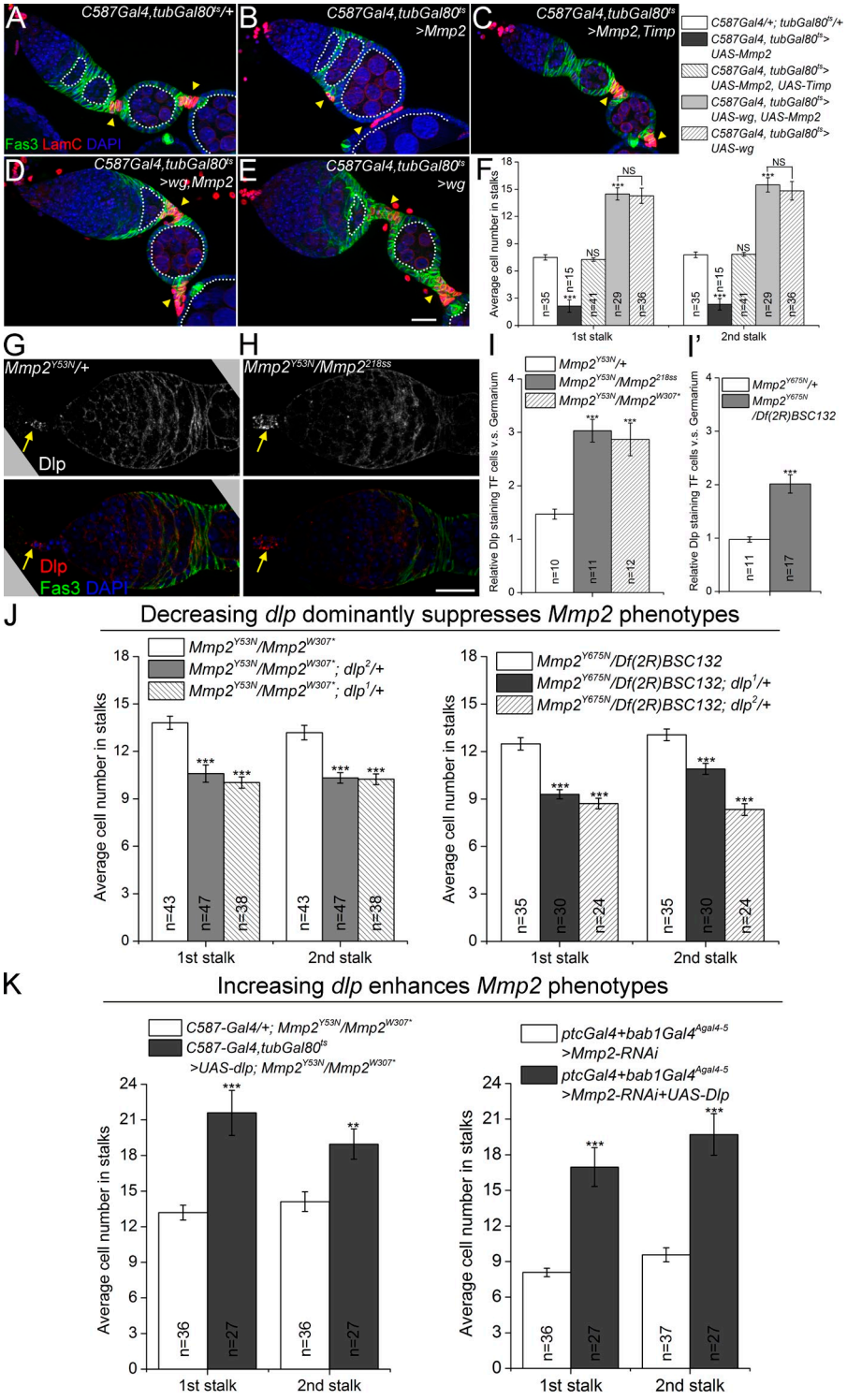

Figure 3. **Mmp2 negatively regulates Dlp to restrict long-range Wg signaling to FSCs.** (A–F) *wg* overexpression is epistatic to *Mmp2* overexpression. *Mmp2* overexpression caused fused egg chambers in 100% of 19 ovarioles examined (B), which was suppressed by co-expression of the Mmp2 catalytic inhibitor, Timp (C). Co-expression of *wg* and *Mmp2* suppressed the *Mmp2* phenotype, with fused egg chambers observed in 9.8% of 51 ovarioles (D). (E) Co-expression of *Mmp2* and *wg* increased stalk cell numbers, phenocopying *wg*-alone overexpression. 16-cell germline cysts are outlined. (F) Quantification of stalk cell numbers. Significances were relative to control (*C587Gal4/+; tubGal80^{ts}/+*) unless otherwise specified. (G–I) *Mmp2* ts mutants showed changes in anti-Dlp staining in the germarium. Note the accumulation of Dlp in TF cells in *Mmp2* mutants (H, arrows). Samples were not permeabilized. Quantification of Dlp localization change is shown in I and I′. (J) Two alleles of *dlp* dominantly suppressed stalk cell increases in *Mmp2* ts mutants. Left: *Mmp2^{Y53N}* trans-heterozygotes. Right: *Mmp2^{Y675N}* trans-heterozygotes. (K) *Dlp* overexpression in escort cells enhances *Mmp2* phenotypes. Left: *Mmp2^{Y53N}* trans-heterozygotes. Right: *Mmp2* RNAi. **, P < 0.01; ***, P < 0.001 (Student's *t* test). Error bars represent SEM. *n* = number of germaria counted or imaged. Bars, 20 µm.

of a "middleman" between Mmp2 and Wg, we did not observe cleavage of Wg protein by Mmp2 in cell culture (Fig. S5 A).

Because Mmp2 negatively regulated Wg signaling, and Dlp promoted Wg signaling, we next asked if *Mmp2* negatively regulated Dlp. Supporting this model, anti-Dlp immunostaining showed altered protein distribution in *Mmp2* mutants (Fig. 3, G and H). Significantly, in two different *Mmp2* ts mutants the Dlp pattern was altered, resulting in Dlp accumulation in apical cells relative to the rest of the germarium (Fig. 3 H; quantified in Fig. 3, I and I′). To test if Mmp2 negatively regulates Dlp function, we removed one copy of *dlp* from *Mmp2* mutants; in these ovaries, the *Mmp2* phenotype of increased stalk cells was dominantly suppressed by *dlp* (Fig. 3 J). This suppression was specific to *dlp*, as two strong mutant alleles each led to dominant suppression (*dlp^{1}*, a deletion mutant; and *dlp^{2}*, an EMS allele; Kirkpatrick et al., 2004); each was tested in two different *Mmp2* ts backgrounds (Fig. 3 J). Reciprocally, overexpression of *dlp* with *C587-Gal4* enhanced the increases in stalk cell numbers in

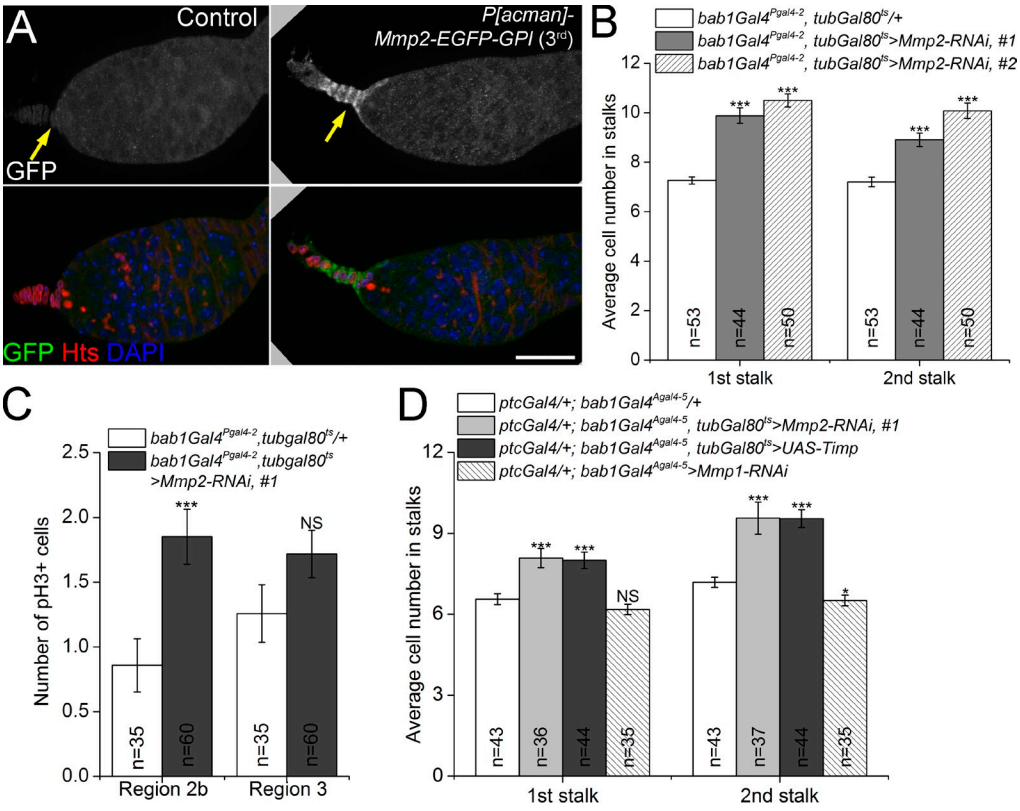

Figure 4. **The FSC niche cells produce a negative regulator of Wg signaling.** (A) Mmp2 protein was localized to apical cells (arrows) by a GFP-tagged BAC genomic construct. Bar, 20 µm. (B) Knocking down *Mmp2* with *bab1Gal4*$^{Pgal4\text{-}2}$ resulted in increased stalk cell numbers. Two RNAi lines targeting different regions of the *Mmp2* ORF gave similar results. (C) Knocking down *Mmp2* with *bab1Gal4*$^{Pgal4\text{-}2}$ resulted in overproliferation of follicle precursor cells in region 2b. (D) The *Mmp2* ts phenotype of increased stalk cell numbers was phenocopied by expressing *Mmp2* RNAi or *Timp*, but not *Mmp1* RNAi, in both apical cells and escort cells. *, $P < 0.05$; ***, $P < 0.001$; NS, not significant (Student's *t* test). Error bars represent SEM. *n* = number of germaria counted.

both an *Mmp2* ts mutant and in an *Mmp2* RNAi knockdown line (Fig. 3 K). Thus, Mmp2 limits Wg signaling and FSC proliferation by antagonizing the function of Dlp.

Mmp2 is required in niche cells

It has not been possible to determine Mmp2 protein localization in any *Drosophila* tissue because no known antibody labels endogenous *Drosophila* Mmp2. To determine Mmp2 protein localization in the ovary, we recombineered a genomic bacterial artificial chromosome (BAC; CH321-81G18) containing *Mmp2* and all endogenous cis-regulatory sequences, including the entire 73-kb *Mmp2* gene region, as well as ∼4 kb in the 3′ direction and ∼17 kb in the 5′ direction (Venken et al., 2008, 2009). The unmodified BAC completely rescued *Mmp2* mutants (unpublished data). We inserted an EGFP sequence before the putative GPI attachment sequence so that the resulting BAC construct (*P[acman]-Mmp2-EGFP-GPI*) expressed EGFP-tagged Mmp2 under endogenous regulatory sequences (Fig. S4 A). After transformation into flies, the Mmp2-EGFP patterns matched those of previously identified in situ hybridization patterns for *Mmp2* (Fig. S4 B; Llano et al., 2002; Page-McCaw et al., 2003). *P[acman]-Mmp2-EGFP-GPI* completely rescued the pupal lethality of *Mmp2* mutants, restoring Mendelian ratios to the progeny classes; however, the lifespan, fertility, and follicle cell phenotypes of adult flies were rescued only in weak allelic combinations (*Mmp2*^{Y53N}*/Df(2R)BSC132*) but not in strong ones (*Mmp2*^{W307*}*/Mmp2*^{218ss}; unpublished data). Given the complete rescue by the untagged *Mmp2* BAC construct, we suspect that the EGFP tag is partially interfering with some Mmp2 functions.

We analyzed the expression pattern of *P[acman]-Mmp2-EGFP-GPI* in the ovary and found that Mmp2-EGFP was expressed most strongly in the apical cells at the anterior of the germarium, which produce the Wg signal, and was also expressed in a few anterior escort cells (Fig. 4 A). Two independent insertions of the construct displayed similar patterns (Fig. S4 C). To determine the cell- and tissue-specific requirements for *Mmp2*, we knocked down *Mmp2* expression with several Gal4 lines expressed in different patterns. When expressed with *bab1Gal4*$^{Pgal4\text{-}2}$ in apical, escort, follicle, and stalk cells (Fig. S4 D), two different *Mmp2-dsRNA* constructs phenocopied the *Mmp2* ts mutants, with significant increases in stalk cell numbers and follicle cell proliferation in region 2b (Fig. 4, B and C). To further refine the requirements for *Mmp2*, we used drivers specific to apical cells (*bab1Gal4*$^{Agal4\text{-}5}$, distinct from the previously described *bab1Gal4*$^{Pgal4\text{-}2}$), escort cells (*ptcGal4*), or follicle cells (*109-30 Gal4*) to knock down *Mmp2*. See Fig. S4 (D–G) for the expression domains of these Gal4 lines. Puzzlingly, none of these resulted in the *Mmp2* phenotype of increased stalk cells (Fig. S4 G, right; and unpublished data). The stalk cell phenotype was recapitulated, however, when we knocked down

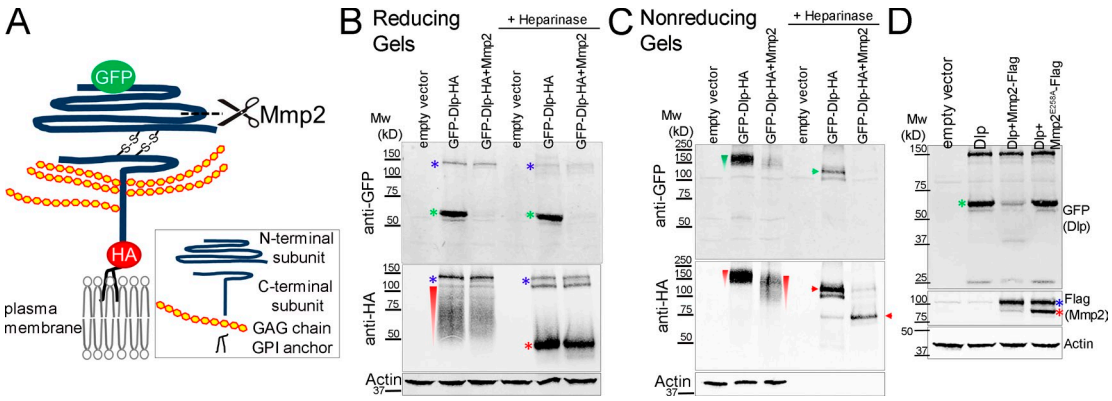

Figure 5. **Mmp2 cleaves the N-terminal subunit of Dlp in cultured cells.** All Western blots were performed on transiently transfected S2R+ cell lysates. (A) Diagram of a Dlp construct. Mature Dlp is processed by furin-like convertase into N- and C-terminal subunits that are linked by two disulfide bonds. GFP labels the N terminus and HA labels the C terminus. The cleavage by Mmp2 as deduced from experiments in B and C is shown. (B) On reducing gels, the N-terminal subunit ran at ∼60 kD (green asterisks); the GAG modifications on the C-terminal subunit caused it to run as a smear (red wedge), resolved by heparinase treatment to a ∼50 kD band (red asterisk). Mmp2 overexpression eliminated detection of the GFP-labeled N-terminal subunit (lanes 3 and 6). The high molecular weight bands (blue asterisk) probably represent unprocessed Dlp precursor polypeptide (see also Fig. S5 C). (C) On nonreducing gels, the disulfide-bonded Dlp protein ran as a smear at ∼150 kD (green and red wedges), resolved by heparinase into doublets (green and red arrow heads) between 100 kD and 150 kD. Mmp2 overexpression reduced the sizes of the Dlp smear (lane 3, red wedge) and band (lane 6, red arrowhead) recognized by HA. (D) Dlp cleavage required Mmp2 catalytic activity, as $Mmp2^{E258A}$ did not decrease the level of GFP-labeled N-terminal subunit (compare lanes 3 and 4). Flag-tagged Mmp2 ran as doublets (the blue asterisk represents the likely zymogen and the red asterisk represents the likely activated enzyme without the pro-domain). Actin, loading control.

Mmp2 in the apical and escort cells simultaneously with both *bab1Gal4*$^{Agal4\text{-}5}$ and *ptcGal4* (Fig. 4 D). Mmp2 catalytic activity is required for FSC proliferation, as expressing the MMP catalytic inhibitor Timp (Page-McCaw et al., 2003; Wei et al., 2003) with the same drivers caused a similar increase in stalk cell numbers (Fig. 4 D). In contrast, knockdown of *Mmp1*, the only other fly MMP, with a functional RNAi (Stevens and Page-McCaw, 2012) did not cause changes in stalk cell number. These results indicate that *Mmp2* is supplied from both apical and escort cells to regulate FSC proliferation via its proteolytic activity, and that either population is sufficient. This is the same region where Dlp accumulates in *Mmp2* mutants (Fig. 3, G and H) and where Wg is expressed (Fig. 1 E).

Mmp2 cleaves Dlp

Mmp2 is an extracellular endopeptidase, and both Mmp2 and Dlp are predicted to have GPI anchors. To determine if Mmp2 cleaves Dlp, we coexpressed Mmp2 and Dlp in S2R+ cultured cells (Yanagawa et al., 1998) and examined the electrophoretic mobility of Dlp. Like mammalian glypicans, Dlp is obligately cleaved by a furin-like pro-protein convertase into two subunits that remain connected by disulfide bonds. The C-terminal subunit contains all the predicted heparan sulfate glycosaminoglycan (GAG) attachment sites (De Cat et al., 2003; Eugster et al., 2007; Kim et al., 2011). We obtained a Dlp construct where the N terminus was tagged with GFP at G69, and the C terminus was tagged with HA at S732 proximal to the GPI anchoring site, allowing us to visualize both subunits (Kreuger et al., 2004; Fig. 5 A). When lysates from cells expressing this Dlp construct were immunoblotted from reducing gels, which disrupted the disulfide bridge, anti-GFP recognized the N-terminal subunit at ∼60 kD (green asterisks in Fig. 5 B), in agreement with previous observations (Eugster et al., 2007), whereas anti-HA recognized the C-terminal subunit as a smear caused by the heterogeneity of the GAG modifications (red wedge in Fig. 5 B). Heparinase treatment removed the GAG modifications and resolved the smear into a band at ∼50 kD (red asterisks in Fig. 5 B). Two faint Dlp bands were observed between 100 and 150 kD (Fig. 5 B, blue asterisks), which probably represent unprocessed Dlp (Fig. S5 C).

Strikingly, when Mmp2 was coexpressed with Dlp, the N-terminal band was nearly eliminated (Fig. 5 B, green asterisks, compare lanes 2 and 3, and lanes 5 and 6). In contrast, neither the mobility nor the abundance of the C-terminal band was affected (Fig. 5 B, red wedge and red asterisk). On nonreducing gels where the subunits remain associated, the HA-tagged Dlp smear exhibited increased mobility in the presence of Mmp2 (Fig. 5 C, compare the red wedges in lanes 2 and 3); when heparinase treatment was applied to resolve the smear, the predominant ∼115-kD HA-tagged band shifted to ∼75 kD in the presence of Mmp2 (Fig. 5 C, compare the red arrowheads). These results indicate that Mmp2 cleaves the N-terminal subunit of Dlp, removing a GFP-containing piece of ∼40 kD. Adjusting for the GFP tag, it appears that Mmp2 cleaves Dlp ∼10–15 kD, or ∼100–140 amino acids, after the signal sequence. A similar loss of the N-terminal Dlp band was observed when the N terminus was tagged with Myc, thus ruling out the possibility that Mmp2 was cleaving the GFP moiety itself (Fig. S5, D and D′). Further supporting the model that Mmp2 cleaves Dlp, we found that a catalytically inactive mutant, $Mmp2^{E258A}$, did not alter Dlp mobility (Fig. 5 D). These data show that Mmp2 is responsible for cleaving Dlp and suggest that the cleaved N-terminal Dlp fragment is either unstable or shed outside the cell. Because Mmp2 and Dlp were overexpressed proteins in these cell culture experiments, we cannot rule out the possibility that one or both are localized to an ectopic location or have lost specificity in some way. However, our cell culture result finding that Mmp2 cleaves Dlp is consistent with our in vivo data showing

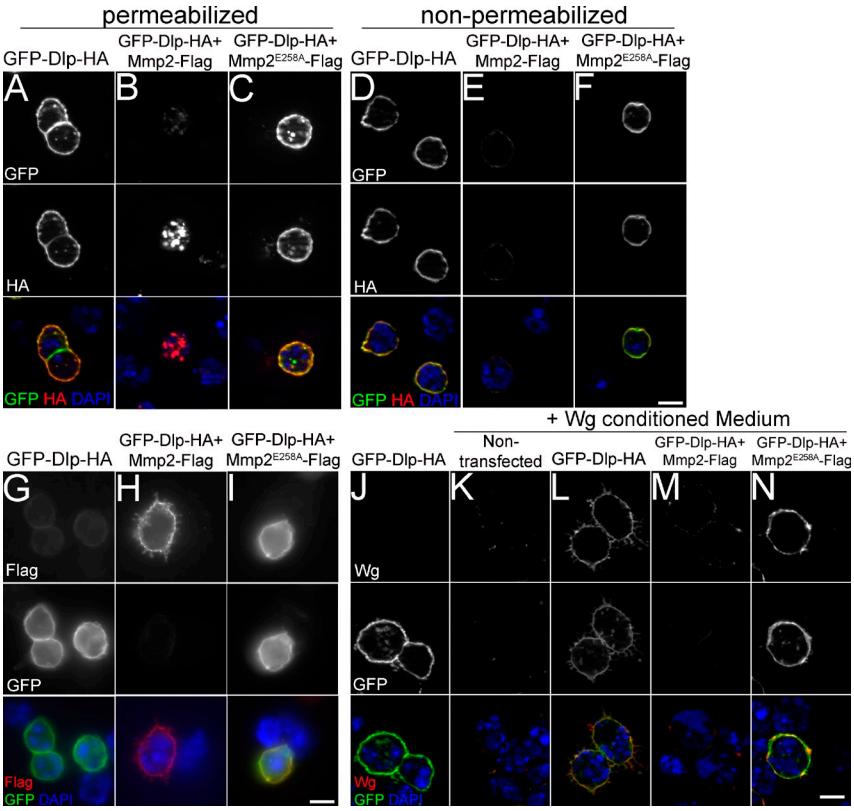

Figure 6. **Mmp2 negatively regulates the cell surface localization of Dlp and reduces Wg binding.** (A–F) Dlp localization was analyzed in S2R+ cells transiently transfected with Dlp labeled by N-terminal GFP and C-terminal HA (see Fig. 5 A), in the absence or presence of Mmp2-Flag or catalytically inactive Mmp2^{E258A}-FLAG. Cell-surface localization of Dlp revealed by anti-GFP and anti-HA staining under permeabilized (A) and nonpermeabilized conditions (D). Dlp coexpression with active Mmp2 caused the loss of the Dlp N terminus labeled by GFP (B and E, top); in the presence of Mmp2, the Dlp C terminus labeled with HA was no longer present on the cell surface (E, middle) but instead was detected inside the cell (B, middle), dependent on Mmp2 catalytic activity (C and F). (G–I) Mmp2 localized to the surface of S2R+ cells, shown in nonpermeabilized cells by anti-Flag staining (H, top). Inactive Mmp2^{E258A} colocalized with Dlp on the cell surface (I). (J–N) Transfected S2R+ cells were incubated with Wg-conditioned media. Wg was detected by anti-Wg, and Dlp was detected by anti-GFP in nonpermeabilized cells. Wg accumulation at the cell surface was Dlp dependent (K and L) and inhibited by active Mmp2 coexpression (M and N). Bars, 10 µm.

that reducing the level of *dlp* attenuates *Mmp2* loss-of-function phenotypes (Fig. 3 J) and that in *Mmp2* mutants Dlp protein accumulates excessively (Fig. 3 H).

Another glypican, Dally, is known to alter the spread of Wg in the wing disc (Han et al., 2005), and Dally is expressed in the germarium where it functions to maintain GSCs (Guo and Wang, 2009; Hayashi et al., 2009). We considered the possibility that Mmp2 may also cleave Dally, but in S2R+ cells we did not observe proteolysis of Dally upon cotransfection with Mmp2 (Fig. S5 B). Consistent with the lack of cleavage, the *Mmp2* phenotype of increased stalk cells does not seem related to the *dally* phenotype of germline loss. Thus we conclude that Dally is not a target of Mmp2 in regulating FSCs.

Mmp2-dependent cleavage inhibits Dlp localization on the cell surface

To determine how Mmp2 cleavage modifies Dlp function, we examined the subcellular distribution of Dlp. When expressed in S2R+ cells, Dlp localized predominantly to the outside of the plasma membrane, with staining visible under permeabilizing and nonpermeabilizing conditions (Fig. 6, A and D). However, when Mmp2 was coexpressed, the cell surface staining of Dlp was dramatically reduced (Fig. 6 E), replaced by prominent intracellular localization visible only under permeabilizing conditions (Fig. 6 B). The loss of Dlp from the cell surface was dependent on the catalytic activity of Mmp2 (Fig. 6, C and F). Interestingly, Mmp2 localized to the outside of the plasma membrane (Fig. 6 H), which suggests that Dlp could interact with Mmp2 on the plasma membrane. When catalytically inactive Mmp2^{E258A} was coexpressed with Dlp, colocalization was detected (Fig. 6 I). Dlp has been shown to bind Wg on the cell surface (Yan et al., 2009), so we next tested if Dlp was capable of binding the Wg ligand after cleavage by Mmp2. Wg accumulation on the cell surface was dependent on Dlp (Fig. 6, K and L), and this accumulation was greatly compromised by coexpression of Mmp2 (Fig. 6 M) but not inactive Mmp2^{E258A} (Fig. 6 N). The lack of Wg binding seems likely to be caused by the loss of Dlp from the cell surface; it is also possible that the Wg-binding domain of Dlp has been disrupted, as Dlp binds Wg through its N-terminal domain (Yan et al., 2009). By cleaving Dlp, Mmp2 limits the capacity of Wg to bind to a protein that promotes its extracellular distribution and protects it from internalization and degradation (Marois et al., 2006; Yan and Lin, 2009). Thus, in the absence of Mmp2, excess Wg signals FSC proliferation.

Discussion

Wnt ligands act in both a short-range and long-range manner. In the fly ovary, it has been known that FSCs lie ∼50 µm from the Wg source at the anterior tip of the germarium (Forbes et al., 1996b; Song and Xie, 2003), which places them as long-range Wg signaling targets. We observed that Wg is produced in cap cells and spreads extracellularly in a visible path extending to the FSCs in wild-type germaria. Although a recent study suggests that Wg may be produced by escort cells, this population of Wg ligand cannot be visualized and at most represents a small fraction of the Wg ligand expressed by cap cells (Sahai-Hernandez and Nystul, 2013). We directly visualized extracellular Wg ligand as specific antibody staining that extends from

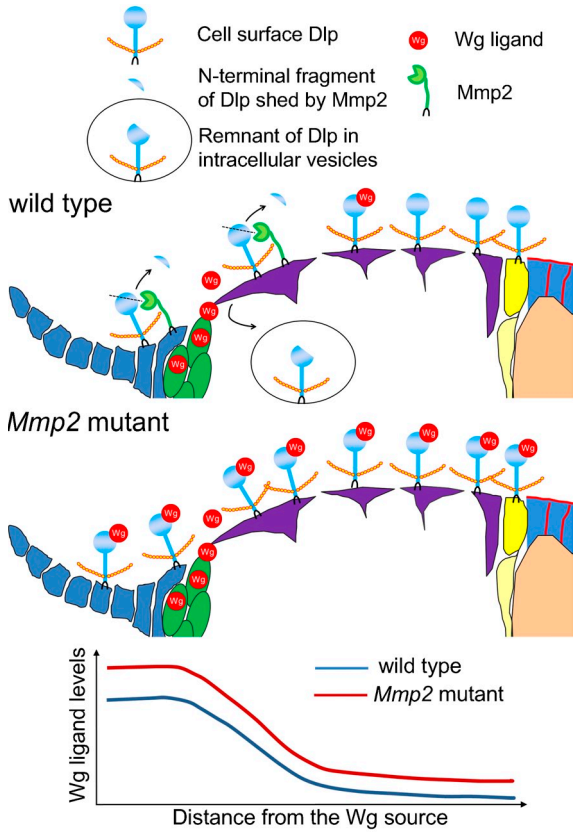

Figure 7. **Model for how Mmp2 regulates Dlp and the distribution of Wg ligand in the germarium.** In the wild-type germarium, Mmp2 is produced near the Wg source (cap cells) and mediates Dlp cleavage caused by the relocalization of Dlp from cell surface to intracellular vesicles. In *Mmp2* mutants, more Dlp is retained at the cell surface to stabilize and facilitate Wg transport, resulting in increased levels of extracellular Wg ligand across the germarium and increased follicle cell divisions.

the cap cells to the FSCs, and we observed a parallel domain of activity with a Wg signaling reporter.

We find that Mmp2 limits the Wg range in the germarium. The range of Wg spreading is controlled by interactions between Wg and Dlp on the cell surface. Our results are consistent with Dlp having the same function in the germarium as it does in the wing disc, where Dlp retains Wg on the cell surface and protects Wg from endocytosis and degradation or from extracellular loss (Marois et al., 2006; Yan and Lin, 2009). Based on our fly and cell culture data, we propose that Mmp2 cleaves Dlp near the Wg source, causing Dlp to relocalize inside the cell where it can no longer interact with or protect extracellular Wg. In wild-type ovaries, Mmp2 serves to limit Wg signaling and FSC proliferation. In *Mmp2* mutants, we observed increased Wg protein levels and a distribution extending further toward the stem cells, and we show that increased stem cell proliferation is dependent on the dose of *wg* in *Mmp2* mutants. Our model of how Mmp2 cleaves Dlp to limit Wg stem cell signaling is sketched in Fig. 7; this model is supported by the following observations. First, Mmp2 cleaves Dlp and induces its loss from the cell surface to an intracellular location in cultured cells. Second, in the ovary, Dlp is required for long-range Wg signaling, and reducing *Dlp* attenuates *Mmp2* loss-of-function stem cell proliferation phenotypes. Third, *Mmp2* mutants exhibit accumulation of Dlp at apical cells, sites where *Mmp2* is expressed.

It would seem that Wg signaling to FSCs could be controlled more easily by altering the level of released ligand. What could be the advantage of these cells expressing Mmp2 as a negative regulator of Wg signaling? Interestingly, we do not find a role for Mmp2 in Wg signaling in the wing disc (unpublished data, see Materials and methods). In the wing disc, Notum appears to play a similar role to Mmp2. Notum antagonizes Dlp by cleaving the GPI anchor from Dlp, and like Mmp2, it is expressed in the Wg domain. Notum appears to act as a feedback regulator of Wg, and Mmp2 may also play this role in the germarium. Alternatively, the role of Mmp2 may reflect differences between the germarium and the wing disc in size regulation. Unlike the wing, which is highly stereotyped in terms of size regulation, the germarium changes size during development, probably cyclically with the production of new egg chambers; the distance between the Wg source and the FSCs changes with it. When the germarium is bigger, the cell surface concentration of Mmp2 and Dlp may be reduced, resulting in fewer cleavage events and more Wg spreading, able to reach the more distant FSCs; conversely, when the germarium is smaller, more cleavage events may limit the spread of Wg to the closer FSCs. Another possibility is that Mmp2 may act to coordinate the development of follicle epithelium with the development of the germline, two tissues that arise from distinct ovarian stem cells that appear to be regulated by niche signals emanating from the same cell types (Li and Xie, 2005).

Implications for other tissues

It has been known that Dlp function is controlled at multiple levels, including transcription, shedding from cell surface, and intracellular trafficking (Baeg et al., 2004; Kreuger et al., 2004; Han et al., 2005; Gallet et al., 2008). Regulatory mechanisms have been identified that govern transcription (Han et al., 2005) and shedding by the lipase Notum, which cleaves the GPI anchor (Kreuger et al., 2004), yet no regulatory mechanism controlling trafficking has been previously discovered. Our study unveils a novel mechanism of Dlp regulation: proteolytic cleavage by Mmp2, which causes a change in Dlp localization from the cell surface to intracellular sites. Dlp is known to regulate ligand availability and/or signaling reception in several signaling pathways in *Drosophila* including Hh, BMP, FGF, and JAK/STAT in addition to Wg (Desbordes and Sanson, 2003; Belenkaya et al., 2004; Yan and Lin, 2007; Gallet et al., 2008; Hayashi et al., 2012; Zhang et al., 2013). The region of Dlp cleaved by Mmp2 is highly conserved in mammalian glypicans, and similarly, vertebrate glypicans regulate many signaling pathways including Wnt, BMP, Hh, and FGF (Filmus et al., 2008; Fico et al., 2011). Additionally, human glypicans participate in tumor susceptibility and progression (DeBaun et al., 2001; Capurro et al., 2005; Jakubovic and Jothy, 2007; Fico et al., 2012). Thus, the regulation of Dlp function by Mmp2 may have widespread significance.

MMPs as Wnt regulators

The concept of MMPs regulating both Wnt signaling and stem cell proliferation was recently introduced in a study in the

mouse mammary gland (Kessenbrock et al., 2013). The authors showed that MMP3 can sequester or cleave Wnt5a, a noncanonical Wnt ligand, which acts as an inhibitor of canonical Wnt signaling, resulting in increased canonical Wnt signaling and stem cell function. In contrast, we show that DmMmp2 inhibits canonical Wnt signaling and stem cell proliferation via cleavage of the glypican Dlp. These two distinct mechanisms reflect the versatility of the Wnt signaling machinery and the variety of its outputs. In the mammary gland, the number of mammary stem cells is variable and controlled by Wnt signaling; the architecture of the resulting epithelial ductal structure is variable and reflects the local signaling environment. Generally, Wnt signaling acts in a canonical fashion through β-catenin/Arm to regulate cell cycle or cell fate; Wnt signaling acts in noncanonical fashion to regulate planar cell polarity or alternative transcriptional responses. In the mammary gland, it appears that MMP3 acts as a switch between canonical and noncanonical Wnt signaling. MMP3 may even act as a feedback inhibitor, switching between these two types of Wnt signaling (Kessenbrock et al., 2013).

The biology of the *Drosophila* ovary reflects different aspects of Wnt signaling. The Wg signal emanates from cells that are 50 µm away from the FSCs, raising the possibility that many cells may respond to the Wg gradient at different concentrations. Indeed, Wg is known to act in a concentration-dependent manner, morphogen-style, so that short-range and long-range targets have distinct signaling responses. The FSCs are long-range Wg targets; closer targets exist for the apical cell Wg signal, as indicated by our Wg reporter *Fz3*. In this tissue, DmMmp2 acts to tune the levels of Wg ligand, regulating the Wg concentration that reaches the FSCs to trigger proliferation. Perhaps Mmp2 in concert with Dlp, which is known to have opposing effects on short-range and long-range targets, acts as a rheostat to selectively alter the strength of signaling to distinct targets along the gradient. In both the mammary gland and in the fly ovary, hyperactive canonical Wnt signaling gives rise to epithelial overgrowth. The results from these two studies highlight not only the diversity of Wnt signaling, but also the need to understand thoroughly the regulatory mechanisms governing Wnt signaling in order to develop effective therapeutic strategies to halt pathological Wnt-driven cell proliferation

DmMmp2 represents a class of MMPs that are attached to the cell surface by a GPI anchor. Two mammalian GPI-anchored MMPs exist, MMP17 and MMP25, and unlike secreted MMPs and MMPs with transmembrane domains, functional studies of this GPI-anchored class of MMPs remain very limited. The GPI anchor is expected to confer MMPs with a unique subcellular localization and offer access to distinct substrates (Sohail et al., 2008). Our results show that GPI-anchored MMPs do indeed play a unique role, as DmMmp2 is not redundant with or compensated by the other *Drosophila* MMP, the secreted Mmp1 (Page-McCaw et al., 2003); and our finding of a GPI-anchored substrate, Dlp, supports the concept that GPI-anchored MMPs have unique substrates based on their cellular localization. Although other heparan sulfate proteoglycans including syndecan are known targets of MMP-mediated proteolysis (Li et al., 2002; Page-McCaw et al., 2007), glypicans have not been previously identified as MMP substrates in any system.

Mammalian MMPs are up-regulated in cancer, and they are considered to promote tumor progression in various stages from initiation to metastasis. The protumorigenic function of MMP3 in breast cancer may involve its activating role in mammary stem cells (Kessenbrock et al., 2013). However, the roles of MMPs in cancer are further complicated by studies that indicate that some MMP family members have tumor-suppressor, protective activities (Decock et al., 2011). Our studies showing that Mmp2 inhibits proliferation of somatic stem cells may advance our understanding of the protective roles of MMPs in cancer.

Materials and methods

Fly stocks

Flies were maintained on cornmeal-molasses media at 25°C. Females harvested for ovaries were fed with fresh wet yeast changed every other day until dissection. Ts alleles of *Mmp2* were generated by treating *cn bw sp* males with 25 mM EMS and selecting for lethal noncomplementation of an *Mmp2* P-insertion at 29°C (Page-McCaw et al., 2003). All *Mmp2* mutant alleles were backcrossed to w^{1118} for four to five generations.

The following stocks are described in Flybase and obtained from Bloomington Drosophila Stock Center: *Df(2R)BSC132*, wg^{CX4}, wg^{IG22}, arm^{2}, *UAS-wg-HA*, *UAS-dlp*, $bab1Gal4^{Pgal4\text{-}2}$ (#6803), $bab1Gal4^{Agal4\text{-}5}$ (#6802), *bab1Gal4* (FBal0242651; provided by A. Gonzalez-Reyes, Universidad Pablo de Olavide, Sevilla, Spain; Bolívar et al., 2006), *ptcGal4* (#2017), and $tubGal80^{ts}$. Other lines include $Mmp2^{02353}$ (FBal0007998), *UAS-Timp* (FBal0150584), *UAS-Mmp2* (FBal0150748; Page-McCaw et al., 2003), *wg-lacZ* (FBal0042267; a gift from G. Struhl, Columbia University, New York, NY); *C587-Gal4* (FBal0150629; a gift from D. Drummond-Barbosa, Johns Hopkins University, Baltimore, MD), *fz3-RFP* (FBal0267159; provided by R. DasGupta, New York University, New York, NY; Olson et al., 2011), dlp^{1} (FBal0190800), and dlp^{2} (FBal0191142; both provided by S. Selleck, Pennsylvania State University, University Park, PA; Kirkpatrick et al., 2004). RNAi lines used were *dlp-RNAi* (Vienna Drosophila RNAi Center, 10299), *wg-RNAi* (#4889R-4), and *Mmp2-RNAi* #1 (#1794-1R-1, both from National Institute of Genetics Fly Stock Center, Japan); as well as *Mmp2-RNAi*, #2 (Transgenic RNAi project, JF01337), and *Mmp1-RNAi* (FBal0212915; Uhlirova and Bohmann, 2006).

Detailed genotypes of animals in each experiment

Figure 1. (B) w^{1118}*; wg-RNAi/+.* (C) *w/*w^{1118}*; wg-RNAi/+; hsGal4/+.* (D) *w; bab1Gal4/UAS-wg-HA.* (E) w^{1118}*; wglacZ/CyO.* (F) *w;* $bab1Gal4^{Agal4\text{-}5}$*,* $tubGal80^{ts}$*/+.* (G) *y w/w hsFlp; X15-33/X15-29.* (H) w^{1118}*; UAS-dlp/+.* (I) *w C587Gal4/w; UAS-Dcr2/UAS-mCD8GFP.* (J) *w C587Gal4/w; UAS-Dcr2/UAS-mCD8GFP; dlp-RNAi/+.* (L) *w C587Gal4/w; fz3-RFP/+.* (M) *w C587Gal4/w; fz3-RFP/UAS-Dcr2; dlp-RNAi/+.* (N) *w; UAS-Dcr2/+; tubGal4,* $tubGal80^{ts}$*/+.* (O) *w; UAS-Dcr2/+; tubGal4,* $tubGal80^{ts}$*/dlp-RNAi.*

Figure 2. (A–C and F) All mutants and heterozygote controls were in a w^{1118} background. (D″) Control, *y w/w hsFlp; X15-33,* $Mmp2^{Y53N}$*/X15-29.* Mutant, *y w/w hsFlp; X15-33,* $Mmp2^{Y53N}$*/X15-29,* $Mmp2^{W307*}$*.* (E) *hsflp/+; FRT13A ubiGFP/FRT13A* $Mmp2^{W307*}$*.* (G) Control, w^{1118}*;* $Mmp2^{Y53N}$*/fz3-RFP.* Mutant, w^{1118}*;* $Mmp2^{Y53N}$*/fz3-RFP,* $Mmp2^{W307*}$*.* (H and I) All genotypes were in a w^{1118} background. (J) From left to right: w^{1118}*;* $Mmp2^{Y53N}$*/+.* w^{1118}*;* $Mmp2^{Y53N}$*/*$Mmp2^{W307*}$*.* arm^{2} *FRT101/*w^{1118}*;* $Mmp2^{Y53N}$*/* $Mmp2^{W307*}$*.*

Figure 3. (A) *w C587Gal4/w;* $tubGal80^{ts}$*/+.* (B) *w C587Gal4/w;* $tubGal80^{ts}$*/UAS-Mmp2.* (C) *w C587Gal4/w; UAS-Timp,* $tubGal80^{ts}$*/UAS-Mmp2.* (D) *w C587Gal4/w;* $tubGal80^{ts}$*/UAS-Mmp2, UAS-wg-HA.* (E) *w C587Gal4/w;* $tubGal80^{ts}$*/UAS-wg-HA.* (G–I′) All mutants and heterozygote controls were in a w^{1118} background. (J, left) From left to right: w^{1118}*;* $Mmp2^{Y53N}$*/*$Mmp2^{W307*}$*.* w^{1118}*;* $Mmp2^{Y53N}$*/*$Mmp2^{W307*}$*; ru h* dlp^{2} *st* ry^{506} *es/+.* w^{1118}*;* $Mmp2^{Y53N}$*/*$Mmp2^{W307*}$*;* dlp^{1} *st*^{1} ry^{506}*/+.* (J, right) From left to right: w^{1118}*;* $Mmp2^{Y675N}$*/Df(2R)BSC132.* w^{1118}*;* $Mmp2^{Y675N}$*/Df(2R)BSC132;* dlp^{1} *FRT2A/+.* w^{1118}*;* $Mmp2^{Y675N}$*/Df(2R)BSC132; ru h* dlp^{2} *st* ry^{506} *es/+.* (K, left, from left to right) *w C587Gal4/*w^{1118}*;* $Mmp2^{Y53N}$*/*$Mmp2^{W307*}$*. w C587Gal4/*w^{1118}*;* $Mmp2^{Y53N}$*/*$Mmp2^{W307*}$*,* $tubGal80^{ts}$*, UAS-dlp/+.* (K, right, from left to right) *w; ptcGal4/+;* $bab1Gal4^{Agal4\text{-}5}$*/Mmp2-RNAi. w; ptcGal4/+;* $bab1Gal4^{Agal4\text{-}5}$*/Mmp2-RNAi, UAS-dlp.*

Figure 4. (A, left) *y w; VK33* (Control). (A, right) *y w; P{P[acman]-Mmp2-EGFP-GPI}VK33.* (B) From left to right: *w;* $bab1Gal4^{Pgal4\text{-}2}$*,* $tubGal80^{ts}$*/+. w;* $bab1Gal4^{Pgal4\text{-}2}$*,* $tubGal80^{ts}$*/UAS-Mmp2-RNAi, #1. w;* $bab1Gal4^{Pgal4\text{-}2}$*,*

tubGal80^{ts}/UAS-Mmp2-RNAi, #2. (C) From left to right: *w; bab1Gal4$^{Pgal4-2}$, tubGal80^{ts}/+. w; bab1Gal4$^{Pgal4-2}$, tubGal80^{ts}/UAS-Mmp2-RNAi, #1*. (D) *w; ptcGal4/+; bab1Gal4$^{Agal4-5}$/+. w; ptcGal4/+; bab1Gal4$^{Agal4-5}$, tubGal80^{ts}/Mmp2-RNAi, #1. w; ptcGal4/+; bab1Gal4$^{Agal4-5}$, tubGal80^{ts}/UAS-Timp. w; ptcGal4/+; bab1Gal4$^{Agal4-5}$/Mmp1-RNAi*.

Clonal analysis and temperature shift conditions

lacZ-labeled mitotic stem-cell clones were generated using previously published methods (Harrison and Perrimon, 1993). The *yw, P[(hsFlp)^{12}, ry^{+}]; X.15.29* and *yw; X.15.33* lines (a gift from N. Perrimon, Harvard Medical School, Boston, MA) were recombined with different *Mmp2* mutant alleles. Flies were collected every 2 d upon eclosion, aged at 29°C for 5 d, exposed to a 1-h heat shock at 37°C, and dissected 7 d later. GFP-negative mitotic clones were generated using FLP-mediated mitotic recombination (Xu and Rubin, 1993). The genotype used was *hsflp/+; FRT13A ubiGFP/FRT13A Mmp2^{W307*}*. 3 d after eclosion, flies were exposed to 1-h heat shocks at 37°C twice a day with an interval of at least 8 h for three consecutive days. Ovaries were dissected 10 d later.

Trans-heterozygous *Mmp2* ts mutant adults were raised at a permissive temperature (18°C for *Mmp2^{Y675N}* and 25°C for *Mmp2^{Y53N}*); progeny were collected upon eclosion every 2 d and shifted to a nonpermissive temperature (29°C) for 7–10 d until dissection. For *Gal4/Gal80^{ts}* controlled gene expression, flies were raised at 18°C, shifted 1–2 d upon eclosion to 29°C, and aged 7–10 d before dissection. For *hs-Gal4* induced expression, 2 d after eclosion flies were heat shocked for 1 h each day for three consecutive days and dissected 3 d later.

Immunohistochemistry

Ovaries were stained as described previously (Song et al., 2002). For nonpermeabilized staining, PBS was used instead of PBST (PBS + 0.1% Triton X-100). Extracellular Wg staining was performed according to a published protocol (Strigini and Cohen, 2000). In brief, dissected ovaries were incubated with anti-Wg (1:3) on ice for 40 min, rinsed thoroughly with cold PBS, and then fixed and costained according to conventional ovary staining procedures. Antibodies used were as follows: mouse anti-Dlp (against Dlp V523-Q702, clone 13G8, 1:5), mouse anti-Fas3 (7G10, 1:8), mouse anti-Hts (1B1, 1:5), mouse anti-lacZ (40-1a, 1:50), mouse anti-LamC (LC28.26, 1:20), mouse anti-Wg (4D4, 1:3), and rat anti-Vasa (1:10). These antibodies were from Developmental Studies Hybridoma Bank (DSHB). Other primary antibodies used were rabbit anti–phospho-Histone H3 (1:1,000; EMD Millipore), mouse anti-GFP (clone N86/38, used 1:5; UC Davis/National Institutes of Health NeuroMab Facility). Secondary antibodies used were Cy3- or FITC-conjugated goat anti–mouse IgG1 or IgG2a, Dylight 649–conjugated donkey anti–rat IgG (all from Jackson ImmunoResearch Laboratories, Inc.), goat anti–rabbit IgG, and goat anti–rat IgG conjugated to Alexa Fluor 488 (Molecular Probes). Stained samples were mounted in Vectashield (Vector Laboratories).

Analysis of Wg signaling in the wing disc

To determine if Mmp2 affects Wg signaling in the wing disc, the following assays were performed. Extracellular Wg was assessed by staining (as described for ovaries) third instar wing discs from *Mmp2^{W307*}/+* and *Mmp2^{W307*}/Mmp2^{218ss}* larvae. The long-range Wg target Dll (Duncan et al., 1998) was assessed by anti-Dll staining of wing discs from *w^{1118}* and *Mmp2^{W307*}/Df(2R)BSC132* third instar larvae. For short-range Wg signaling, *Mmp2* ts mutants (*Mmp2^{Y53N}/Df(2R)BSC132* and *Mmp2^{Y53N}/Mmp2^{W307*}*) were raised at 29°C for 5 d until pupariation, shifted to 25°C for 2 d, and then shifted back to 29°C through eclosion. Mechanosensory bristles on the wing margin were counted as an indicator of short-range Wg signaling. No differences were observed between control and *Mmp2* mutants in any of these assays.

Plasmids and recombineering

pUAST-Mmp2-Flag was constructed from pUAST-Mmp2 (Page-McCaw et al., 2003) by introducing a BamHI site into Mmp2 (after S710) and subsequently inserting a 3× flag sequence flanked by BamHI sites. The E258A mutation was introduced by PCR into pUAST-Mmp2-Flag to generate pUAST-Mmp2^{E258A}-Flag. Other plasmids used were pUAST-GFP-Dlp-HA-C (GFP was inserted in place of G69 via SphI and the HA tag was inserted at S732 via NheI into Dlp; provided by S. Cohen, Institute of Molecular and Cell Biology, Singapore; Kreuger et al., 2004), pAW-Dally-Myc (Myc was inserted at R50 via Aat II into Dally; provided by H. Nakato, University of Minnesota, Minneapolis, MN; Dejima et al., 2011), and pMT-Gal4 (FBmc0003005).

A genomic BAC construct for *Mmp2* (CH321-81G18, 2R:9,607,564–9,701,338, Berkeley Drosophila Genome Project *D. melanogaster* Release_6) was obtained from the P[acman] libraries (Venken et al., 2009). To construct P[acman]-Mmp2-EGFP-GPI, an EGFP tag was inserted before the GPI anchor of Mmp2 (after S710) by recombineering using PL-452 C-EGFP as the template vector (Venken et al., 2008). Transgenic flies were generated for both untagged and tagged Mmp2 BAC constructs by φC31-mediated integration into *yw; attP40; VK33* flies (Genetic Services Inc.). Integration events were identified by screening for w+ and confirmed by PCR.

Cell culture, transfection, and immunoblotting

Drosophila S2 cells (Drosophila Genomics Resources Center) and S2R+ cells (a gift of N. Perrimon) were maintained at 27°C in Schneider's *Drosophila* medium (Gibco) containing 10% heat inactivated fetal bovine serum (BRL 16140; Gibco) and 100 U/ml penicillin/streptomycin. Transient transfection was performed as described previously (Broderick et al., 2012). Induction of protein expression was performed in the presence of 0.7 mM Cu^{2+} at 27°C for 2 d; or for any Dlp or Dally-related experiments, at 18°C for 4 d to promote better processing and folding of Dlp.

For immunoblotting, cell pellets were washed in PBS, resuspended in 1× NuPage LDS sample buffer (Invitrogen) with (for reducing gels) or without (for nonreducing gels) 5% β-mercaptoethanol, and heated at 75°C for 5 min. Lysates were run on 10% Mini-PROTEAN TGX precast gels (Bio-Rad Laboratories) and transferred onto Hybond-C Extra nitrocellulose membranes (GE Healthcare). Blots were probed with primary antibodies including rabbit anti-GFP (ab6556; Abcam), mouse anti-GFP (clones 7.1 and 13.1; Roche), rat anti-HA (3F10; Roche), anti-actin (MAB1501R; EMD Milllipore), and rabbit anti-Flag (F7425; Sigma-Aldrich). Secondary antibodies used were: donkey anti–rabbit or anti–mouse IgG conjugated to IRDye 680, and goat anti–rat IgG conjugated to IRDye 680 or IRDye 800CW (LI-COR Biosciences). Blots were developed and imaged with the Odyssey Infrared Imaging System (LI-COR Biosciences).

For immunostaining, S2R+ cells were harvested, reattached to a 12-well multi-test slide (MP Biomedicals), and stained as described previously (Broderick et al., 2012). PBST was used to permeabilize cells whereas PBS was used for nonpermeabilized staining. Primary antibodies used were: mouse anti-GFP (clone N86/38, 1:25; UC Davis/National Institutes of Health NeuroMab Facility), rat anti-HA (3F10, 1:500; Roche), mouse anti-Wg (4D4, 1:33; DSHB), and rabbit anti-Flag (1:500; Sigma-Aldrich). Secondary antibodies used were FITC-conjugated goat anti–mouse IgG2a, Dylight 649–conjugated donkey anti–rat, Cy3-conjugated goat anti–mouse IgG1, and Cy3-conjugated donkey anti–rabbit IgG (all from Jackson ImmunoResearch Laboratories, Inc.).

Heparinase treatment

For heparinase treatment, cells were lysed in 50 mM Tris-HCl, pH 7.5, 150 mM NaCl, and 0.5% Triton X-100 plus complete proteinase inhibitor (EDTA free; Roche) on ice for 30 min. Supernatant was diluted with equal volumes of 20 mM Tris-HCl, pH 7.5, and 4 mM $CaCl_2$ plus complete proteinase inhibitor (EDTA free; Roche). Heparinase III (Sigma-Aldrich) was added to a final concentration of 2 U/ml. After 4 h of incubation at 37°C, the reaction was halved and the two aliquots were mixed with NuPage LDS sample buffer (Invitrogen) with (for reducing gels) or without β-ME (for nonreducing gels) and run on 10% Mini-Protean TGX precast gels (Bio-Rad Laboratories).

Wg-binding assay

The Wg binding assay was performed as described previously (Wu et al., 2010). In brief, Wg-conditioned medium was collected from a S2-Tub-wg stable cell line (Drosophila Genomics Resources Center). To assay Wg binding, S2R+ cells were seeded onto poly-D-lysine–coated coverslips (Neuvitro) in a 24-well plate and transfected. After Cu^{2+} induction, cells were prechilled, incubated with Wg-conditioned medium on ice for 3 h, and processed for immunostaining.

Fluorescence microscopy, imaging, and quantification

All samples were imaged by an Axioimager M2 (Carl Zeiss) equipped with an Apotome system and a camera (AxioCam MRm; Carl Zeiss). Images were acquired using 40×/1.3 NA oil EC Plan-NeoFluor or 63×/1.4 NA oil Plan-Apochromat objective lenses at room temperature. The Axiovision 4.8 software (Carl Zeiss) was used for data acquisition, and projections of z stacks were compiled using the Orthoview functions. Images were exported as 16-bit TIF files and processed with Photoshop CS4 (Adobe). Fluorescence intensities were quantified on selected regions of the germarium using the Measure tool of ImageJ 1.45s (National Institutes of Health). For quantification of Wg levels (Figs. 1 K and 2 F′), total intensity

of Wg staining was measured over the area of apical cells and along the basement membrane between the apical cells and the FSCs. Relative intensity was calculated by setting values in control samples to 1. For quantification of fz3-RFP activity (Fig. 2 G′), mean RFP intensity was measured over FSCs and follicle precursor cells in region 2b and relative intensity was calculated by setting the control value to 1. For quantification of Dlp staining (Fig. 3, I and I′), mean intensities were measured over the terminal filament (TF) cell region and over the rest of the germaria, and the ratio of the former to the latter was calculated for each genotype.

Statistics

To determine the number of stalk cells, ovaries were stained with anti-LamC to label the nuclear membrane of stalk cells, then the cell number in the first stalk (posterior to region 3 of the germarium; Fig. 1 A) and the second stalk (posterior to stage 1–2 egg chamber; Fig. 1 A) were counted. To determine the number of dividing follicle cells per germarium, ovaries were stained with anti–phospho-Histone H3, and the number of positively labeled follicle cells in region 2b and region 3 of the germarium (Fig. 1 A) was counted. For lineage analysis in Fig. 2 D, germaria were examined for the presence of GSC or FSC clones positively labeled by lacZ staining, and the percentages containing at least one labeled clone were determined. Mean values were calculated from four independent experiments, and for each experiment, ∼60–100 germaria were scored. Stem cell clones were identified by aging the flies for 7 d after clone induction to allow all transit clones to exit the germaria before dissection. GSC clones were further confirmed by their location (adjacent to cap cells), and FSC clones were confirmed by their low level of Fas3 staining, triangular shape, and location at the border of regions 2a and 2b. A Student's *t* test (two-tailed, two-sample equal variance) was used for statistical analysis and a P-value of <0.05 was considered significant.

Online supplemental material

Fig. S1 shows that extracellular anti-Wg staining in the germaria is specific. Fig. S2 shows the assessment of Wg activity-reporter candidates in the germaria. Fig. S3 describes *Mmp2* mutant alleles and additional phenotypes. Fig. S4 shows Mmp2-EGFP-GPI structure and expression, GAL4 domains, and *Mmp2* knockdown in follicle cells. Fig. S5 show supplementary biochemical analysis in cell culture. Online supplemental material is available at http://www.jcb.org/cgi/content/full/jcb.201403084/DC1.

We thank K. Cadigan, R. DasGupta, D. Drummond-Barbosa, A. Gonzalez-Reyes, N. Perrimon, S. Selleck, G. Struhl, the Bloomington Drosophila Stock Center, TRiP at Harvard Medical School (National Institutes of Health/NIGMS R01-GM084947), National Institute of Genetics Fly Stock Center (Japan), and the Vienna Drosophila RNAi Center for fly stocks; S. Cohen, X. Lin, H. Nakato, and Addgene for plasmids; the Drosophila Genomics Resource Center for cell lines; H. Bellen, I. Duncan, and the Developmental Studies Hybridoma Bank for antibodies. We thank W. Parks, E. Lee, and G. Bhave for suggestions on the biochemistry; K. LaFever for technical support; U. Tepass for ideas; and L. Lee and W. Ramos-Lewis for comments on the manuscript.

This work was supported by National Institutes of Health grants R03 HD074834 and R01 GM073883 to A. Page-McCaw.

The authors declare no competing financial interests.

Submitted: 20 March 2014
Accepted: 27 August 2014

References

Alexandre, C., A. Baena-Lopez, and J.P. Vincent. 2014. Patterning and growth control by membrane-tethered Wingless. *Nature*. 505:180–185. http://dx.doi.org/10.1038/nature12879

Baeg, G.H., E.M. Selva, R.M. Goodman, R. Dasgupta, and N. Perrimon. 2004. The Wingless morphogen gradient is established by the cooperative action of Frizzled and Heparan Sulfate Proteoglycan receptors. *Dev. Biol.* 276:89–100. http://dx.doi.org/10.1016/j.ydbio.2004.08.023

Belenkaya, T.Y., C. Han, D. Yan, R.J. Opoka, M. Khodoun, H. Liu, and X. Lin. 2004. *Drosophila* Dpp morphogen movement is independent of dynamin-mediated endocytosis but regulated by the glypican members of heparan sulfate proteoglycans. *Cell*. 119:231–244. http://dx.doi.org/10.1016/j.cell.2004.09.031

Bolívar, J., J. Pearson, L. López-Onieva, and A. González-Reyes. 2006. Genetic dissection of a stem cell niche: the case of the *Drosophila* ovary. *Dev. Dyn.* 235:2969–2979. http://dx.doi.org/10.1002/dvdy.20967

Broderick, S., X. Wang, N. Simms, and A. Page-McCaw. 2012. *Drosophila* Ninjurin A induces nonapoptotic cell death. *PLoS ONE*. 7:e44567. http://dx.doi.org/10.1371/journal.pone.0044567

Capurro, M.I., Y.Y. Xiang, C. Lobe, and J. Filmus. 2005. Glypican-3 promotes the growth of hepatocellular carcinoma by stimulating canonical Wnt signaling. *Cancer Res.* 65:6245–6254. http://dx.doi.org/10.1158/0008-5472.CAN-04-4244

Clevers, H., and R. Nusse. 2012. Wnt/β-catenin signaling and disease. *Cell*. 149:1192–1205. http://dx.doi.org/10.1016/j.cell.2012.05.012

Cox, R.T., L.M. Pai, C. Kirkpatrick, J. Stein, and M. Peifer. 1999. Roles of the C terminus of Armadillo in Wingless signaling in *Drosophila*. *Genetics*. 153:319–332.

DeBaun, M.R., J. Ess, and S. Saunders. 2001. Simpson Golabi Behmel syndrome: progress toward understanding the molecular basis for overgrowth, malformation, and cancer predisposition. *Mol. Genet. Metab.* 72:279–286. http://dx.doi.org/10.1006/mgme.2001.3150

De Cat, B., S.Y. Muyldermans, C. Coomans, G. Degeest, B. Vanderschueren, J. Creemers, F. Biemar, B. Peers, and G. David. 2003. Processing by proprotein convertases is required for glypican-3 modulation of cell survival, Wnt signaling, and gastrulation movements. *J. Cell Biol.* 163:625–635. http://dx.doi.org/10.1083/jcb.200302152

Decock, J., S. Thirkettle, L. Wagstaff, and D.R. Edwards. 2011. Matrix metalloproteinases: protective roles in cancer. *J. Cell. Mol. Med.* 15:1254–1265. http://dx.doi.org/10.1111/j.1582-4934.2011.01302.x

Dejima, K., M.I. Kanai, T. Akiyama, D.C. Levings, and H. Nakato. 2011. Novel contact-dependent bone morphogenetic protein (BMP) signaling mediated by heparan sulfate proteoglycans. *J. Biol. Chem.* 286:17103–17111. http://dx.doi.org/10.1074/jbc.M110.208082

de Lau, W., N. Barker, and H. Clevers. 2007. WNT signaling in the normal intestine and colorectal cancer. *Front. Biosci.* 12:471–491. http://dx.doi.org/10.2741/2076

Desbordes, S.C., and B. Sanson. 2003. The glypican Dally-like is required for Hedgehog signalling in the embryonic epidermis of *Drosophila*. *Development*. 130:6245–6255. http://dx.doi.org/10.1242/dev.00874

Duncan, D.M., E.A. Burgess, and I. Duncan. 1998. Control of distal antennal identity and tarsal development in *Drosophila* by spineless-aristapedia, a homolog of the mammalian dioxin receptor. *Genes Dev.* 12:1290–1303. http://dx.doi.org/10.1101/gad.12.9.1290

Eugster, C., D. Panáková, A. Mahmoud, and S. Eaton. 2007. Lipoprotein-heparan sulfate interactions in the Hh pathway. *Dev. Cell.* 13:57–71. http://dx.doi.org/10.1016/j.devcel.2007.04.019

Fico, A., F. Maina, and R. Dono. 2011. Fine-tuning of cell signaling by glypicans. *Cell. Mol. Life Sci.* 68:923–929. http://dx.doi.org/10.1007/s00018-007-7471-6

Fico, A., A. De Chevigny, J. Egea, M.R. Bösl, H. Cremer, F. Maina, and R. Dono. 2012. Modulating Glypican4 suppresses tumorigenicity of embryonic stem cells while preserving self-renewal and pluripotency. *Stem Cells*. 30:1863–1874. http://dx.doi.org/10.1002/stem.1165

Filmus, J., M. Capurro, and J. Rast. 2008. Glypicans. *Genome Biol.* 9:224. http://dx.doi.org/10.1186/gb-2008-9-5-224

Flesken-Nikitin, A., C.I. Hwang, C.Y. Cheng, T.V. Michurina, G. Enikolopov, and A.Y. Nikitin. 2013. Ovarian surface epithelium at the junction area contains a cancer-prone stem cell niche. *Nature*. 495:241–245. http://dx.doi.org/10.1038/nature11979

Forbes, A.J., H. Lin, P.W. Ingham, and A.C. Spradling. 1996a. hedgehog is required for the proliferation and specification of ovarian somatic cells prior to egg chamber formation in *Drosophila*. *Development*. 122:1125–1135.

Forbes, A.J., A.C. Spradling, P.W. Ingham, and H. Lin. 1996b. The role of segment polarity genes during early oogenesis in *Drosophila*. *Development*. 122:3283–3294.

Franch-Marro, X., O. Marchand, E. Piddini, S. Ricardo, C. Alexandre, and J.P. Vincent. 2005. Glypicans shunt the Wingless signal between local signalling and further transport. *Development*. 132:659–666. http://dx.doi.org/10.1242/dev.01639

Gallet, A., L. Staccini-Lavenant, and P.P. Thérond. 2008. Cellular trafficking of the glypican Dally-like is required for full-strength Hedgehog signaling and wingless transcytosis. *Dev. Cell.* 14:712–725. http://dx.doi.org/10.1016/j.devcel.2008.03.001

Guo, Z., and Z. Wang. 2009. The glypican Dally is required in the niche for the maintenance of germline stem cells and short-range BMP signaling in the *Drosophila* ovary. *Development*. 136:3627–3635. http://dx.doi.org/10.1242/dev.036939

Han, C., D. Yan, T.Y. Belenkaya, and X. Lin. 2005. *Drosophila* glypicans Dally and Dally-like shape the extracellular Wingless morphogen gradient in the wing disc. *Development*. 132:667–679. http://dx.doi.org/10.1242/dev.01636

Hanahan, D., and R.A. Weinberg. 2011. Hallmarks of cancer: the next generation. *Cell*. 144:646–674. http://dx.doi.org/10.1016/j.cell.2011.02.013

Harrison, D.A., and N. Perrimon. 1993. Simple and efficient generation of marked clones in *Drosophila*. *Curr. Biol.* 3:424–433. http://dx.doi.org/10.1016/0960-9822(93)90349-S

Hayashi, Y., S. Kobayashi, and H. Nakato. 2009. *Drosophila* glypicans regulate the germline stem cell niche. *J. Cell Biol.* 187:473–480. http://dx.doi.org/10.1083/jcb.200904118

Hayashi, Y., T.R. Sexton, K. Dejima, D.W. Perry, M. Takemura, S. Kobayashi, H. Nakato, and D.A. Harrison. 2012. Glypicans regulate JAK/STAT signaling and distribution of the Unpaired morphogen. *Development*. 139:4162–4171. http://dx.doi.org/10.1242/dev.078055

Horne-Badovinac, S., and D. Bilder. 2005. Mass transit: epithelial morphogenesis in the *Drosophila* egg chamber. *Dev. Dyn.* 232:559–574. http://dx.doi.org/10.1002/dvdy.20286

Jakubovic, B.D., and S. Jothy. 2007. Glypican-3: from the mutations of Simpson-Golabi-Behmel genetic syndrome to a tumor marker for hepatocellular carcinoma. *Exp. Mol. Pathol.* 82:184–189. http://dx.doi.org/10.1016/j.yexmp.2006.10.010

Kessenbrock, K., G.J. Dijkgraaf, D.A. Lawson, L.E. Littlepage, P. Shahi, U. Pieper, and Z. Werb. 2013. A role for matrix metalloproteinases in regulating mammary stem cell function via the Wnt signaling pathway. *Cell Stem Cell*. 13:300–313. http://dx.doi.org/10.1016/j.stem.2013.06.005

Kim, M.S., A.M. Saunders, B.Y. Hamaoka, P.A. Beachy, and D.J. Leahy. 2011. Structure of the protein core of the glypican Dally-like and localization of a region important for hedgehog signaling. *Proc. Natl. Acad. Sci. USA*. 108:13112–13117. http://dx.doi.org/10.1073/pnas.1109877108

Kirilly, D., S. Wang, and T. Xie. 2011. Self-maintained escort cells form a germline stem cell differentiation niche. *Development*. 138:5087–5097. http://dx.doi.org/10.1242/dev.067850

Kirkpatrick, C.A., B.D. Dimitroff, J.M. Rawson, and S.B. Selleck. 2004. Spatial regulation of Wingless morphogen distribution and signaling by Dally-like protein. *Dev. Cell*. 7:513–523. http://dx.doi.org/10.1016/j.devcel.2004.08.004

Kreuger, J., L. Perez, A.J. Giraldez, and S.M. Cohen. 2004. Opposing activities of Dally-like glypican at high and low levels of Wingless morphogen activity. *Dev. Cell*. 7:503–512. http://dx.doi.org/10.1016/j.devcel.2004.08.005

Lander, A.D., J. Kimble, H. Clevers, E. Fuchs, D. Montarras, M. Buckingham, A.L. Calof, A. Trumpp, and T. Oskarsson. 2012. What does the concept of the stem cell niche really mean today? *BMC Biol.* 10:19. http://dx.doi.org/10.1186/1741-7007-10-19

Li, L., and T. Xie. 2005. Stem cell niche: structure and function. *Annu. Rev. Cell Dev. Biol.* 21:605–631. http://dx.doi.org/10.1146/annurev.cellbio.21.012704.131525

Li, Q., P.W. Park, C.L. Wilson, and W.C. Parks. 2002. Matrilysin shedding of syndecan-1 regulates chemokine mobilization and transepithelial efflux of neutrophils in acute lung injury. *Cell*. 111:635–646. http://dx.doi.org/10.1016/S0092-8674(02)01079-6

Llano, E., G. Adam, A.M. Pendás, V. Quesada, L.M. Sánchez, I. Santamariá, S. Noselli, and C. López-Otín. 2002. Structural and enzymatic characterization of *Drosophila* Dm2-MMP, a membrane-bound matrix metalloproteinase with tissue-specific expression. *J. Biol. Chem.* 277:23321–23329. http://dx.doi.org/10.1074/jbc.M200121200

Manseau, L., A. Baradaran, D. Brower, A. Budhu, F. Elefant, H. Phan, A.V. Philp, M. Yang, D. Glover, K. Kaiser, et al. 1997. GAL4 enhancer traps expressed in the embryo, larval brain, imaginal discs, and ovary of *Drosophila*. *Dev. Dyn.* 209:310–322. http://dx.doi.org/10.1002/(SICI)1097-0177(199707)209:3<310::AID-AJA6>3.0.CO;2-L

Margolis, J., and A. Spradling. 1995. Identification and behavior of epithelial stem cells in the *Drosophila* ovary. *Development*. 121:3797–3807.

Marois, E., A. Mahmoud, and S. Eaton. 2006. The endocytic pathway and formation of the Wingless morphogen gradient. *Development*. 133:307–317. http://dx.doi.org/10.1242/dev.02197

Niehrs, C. 2012. The complex world of WNT receptor signalling. *Nat. Rev. Mol. Cell Biol.* 13:767–779. http://dx.doi.org/10.1038/nrm3470

Nystul, T., and A. Spradling. 2007. An epithelial niche in the *Drosophila* ovary undergoes long-range stem cell replacement. *Cell Stem Cell*. 1:277–285. http://dx.doi.org/10.1016/j.stem.2007.07.009

Nystul, T., and A. Spradling. 2010. Regulation of epithelial stem cell replacement and follicle formation in the *Drosophila* ovary. *Genetics*. 184:503–515. http://dx.doi.org/10.1534/genetics.109.109538

Olson, E.R., R. Pancratov, S.S. Chatterjee, B. Changkakoty, Z. Pervaiz, and R. DasGupta. 2011. Yan, an ETS-domain transcription factor, negatively modulates the Wingless pathway in the *Drosophila* eye. *EMBO Rep.* 12:1047–1054. http://dx.doi.org/10.1038/embor.2011.159

Page-McCaw, A., J. Serano, J.M. Santé, and G.M. Rubin. 2003. *Drosophila* matrix metalloproteinases are required for tissue remodeling, but not embryonic development. *Dev. Cell*. 4:95–106. http://dx.doi.org/10.1016/S1534-5807(02)00400-8

Page-McCaw, A., A.J. Ewald, and Z. Werb. 2007. Matrix metalloproteinases and the regulation of tissue remodelling. *Nat. Rev. Mol. Cell Biol.* 8:221–233. http://dx.doi.org/10.1038/nrm2125

Rogers, K.W., and A.F. Schier. 2011. Morphogen gradients: from generation to interpretation. *Annu. Rev. Cell Dev. Biol.* 27:377–407. http://dx.doi.org/10.1146/annurev-cellbio-092910-154148

Sahai-Hernandez, P., and T.G. Nystul. 2013. A dynamic population of stromal cells contributes to the follicle stem cell niche in the *Drosophila* ovary. *Development*. 140:4490–4498. http://dx.doi.org/10.1242/dev.098558

Sohail, A., Q. Sun, H. Zhao, M.M. Bernardo, J.A. Cho, and R. Fridman. 2008. MT4-(MMP17) and MT6-MMP (MMP25), A unique set of membrane-anchored matrix metalloproteinases: properties and expression in cancer. *Cancer Metastasis Rev.* 27:289–302. http://dx.doi.org/10.1007/s10555-008-9129-8

Song, X., and T. Xie. 2003. Wingless signaling regulates the maintenance of ovarian somatic stem cells in *Drosophila*. *Development*. 130:3259–3268. http://dx.doi.org/10.1242/dev.00524

Song, X., C.H. Zhu, C. Doan, and T. Xie. 2002. Germline stem cells anchored by adherens junctions in the *Drosophila* ovary niches. *Science*. 296:1855–1857. http://dx.doi.org/10.1126/science.1069871

Stevens, L.J., and A. Page-McCaw. 2012. A secreted MMP is required for reepithelialization during wound healing. *Mol. Biol. Cell*. 23:1068–1079. http://dx.doi.org/10.1091/mbc.E11-09-0745

Strigini, M., and S.M. Cohen. 2000. Wingless gradient formation in the *Drosophila* wing. *Curr. Biol.* 10:293–300. http://dx.doi.org/10.1016/S0960-9822(00)00378-X

Uhlirova, M., and D. Bohmann. 2006. JNK- and Fos-regulated Mmp1 expression cooperates with Ras to induce invasive tumors in *Drosophila*. *EMBO J.* 25:5294–5304. http://dx.doi.org/10.1038/sj.emboj.7601401

Venken, K.J., J. Kasprowicz, S. Kuenen, J. Yan, B.A. Hassan, and P. Verstreken. 2008. Recombineering-mediated tagging of *Drosophila* genomic constructs for in vivo localization and acute protein inactivation. *Nucleic Acids Res.* 36:e114. http://dx.doi.org/10.1093/nar/gkn486

Venken, K.J., J.W. Carlson, K.L. Schulze, H. Pan, Y. He, R. Spokony, K.H. Wan, M. Koriabine, P.J. de Jong, K.P. White, et al. 2009. Versatile P[acman] BAC libraries for transgenesis studies in *Drosophila melanogaster*. *Nat. Methods*. 6:431–434. http://dx.doi.org/10.1038/nmeth.1331

Vied, C., A. Reilein, N.S. Field, and D. Kalderon. 2012. Regulation of stem cells by intersecting gradients of long-range niche signals. *Dev. Cell*. 23:836–848. http://dx.doi.org/10.1016/j.devcel.2012.09.010

Wei, S., Z. Xie, E. Filenova, and K. Brew. 2003. Drosophila TIMP is a potent inhibitor of MMPs and TACE: similarities in structure and function to TIMP-3. *Biochemistry*. 42:12200–12207. http://dx.doi.org/10.1021/bi035358x

Wu, Y., T.Y. Belenkaya, and X. Lin. 2010. Dual roles of *Drosophila* glypican Dally-like in Wingless/Wnt signaling and distribution. *Methods Enzymol.* 480:33–50. http://dx.doi.org/10.1016/S0076-6879(10)80002-3

Xu, T., and G.M. Rubin. 1993. Analysis of genetic mosaics in developing and adult *Drosophila* tissues. *Development*. 117:1223–1237.

Yan, D., and X. Lin. 2007. Drosophila glypican Dally-like acts in FGF-receiving cells to modulate FGF signaling during tracheal morphogenesis. *Dev. Biol.* 312:203–216. http://dx.doi.org/10.1016/j.ydbio.2007.09.015

Yan, D., and X. Lin. 2009. Shaping morphogen gradients by proteoglycans. *Cold Spring Harb. Perspect. Biol.* 1:a002493. http://dx.doi.org/10.1101/cshperspect.a002493

Yan, D., Y. Wu, Y. Feng, S.C. Lin, and X. Lin. 2009. The core protein of glypican Dally-like determines its biphasic activity in wingless morphogen signaling. *Dev. Cell*. 17:470–481. http://dx.doi.org/10.1016/j.devcel.2009.09.001

Yanagawa, S., J.S. Lee, and A. Ishimoto. 1998. Identification and characterization of a novel line of *Drosophila* Schneider S2 cells that respond to wingless signaling. *J. Biol. Chem.* 273:32353–32359. http://dx.doi.org/10.1074/jbc.273.48.32353

Zhang, Y., and D. Kalderon. 2001. Hedgehog acts as a somatic stem cell factor in the *Drosophila* ovary. *Nature*. 410:599–604. http://dx.doi.org/10.1038/35069099

Zhang, Y., J. You, W. Ren, and X. Lin. 2013. *Drosophila* glypicans Dally and Dally-like are essential regulators for JAK/STAT signaling and Unpaired distribution in eye development. *Dev. Biol.* 375:23–32. http://dx.doi.org/10.1016/j.ydbio.2012.12.019